

# RSC Advances



This is an *Accepted Manuscript*, which has been through the Royal Society of Chemistry peer review process and has been accepted for publication.

*Accepted Manuscripts* are published online shortly after acceptance, before technical editing, formatting and proof reading. Using this free service, authors can make their results available to the community, in citable form, before we publish the edited article. This *Accepted Manuscript* will be replaced by the edited, formatted and paginated article as soon as this is available.

You can find more information about *Accepted Manuscripts* in the [Information for Authors](#).

Please note that technical editing may introduce minor changes to the text and/or graphics, which may alter content. The journal's standard [Terms & Conditions](#) and the [Ethical guidelines](#) still apply. In no event shall the Royal Society of Chemistry be held responsible for any errors or omissions in this *Accepted Manuscript* or any consequences arising from the use of any information it contains.

1 **Title:** Dispersive and FT-Raman spectroscopic methods in Food Analysis

2

3 **Authors:** Ismail Hakki Boyacı<sup>1,2\*</sup>, Havva Tümay Temiz<sup>1</sup>, Hüseyin Efe Geniş<sup>1</sup>, Esra Acar  
4 Soykut<sup>2</sup>, Nazife Nur Yazgan<sup>1</sup>, Burcu Güven<sup>1</sup>, Reyhan Selin Uysal<sup>1</sup>, Akif Göktuğ Bozkurt<sup>1</sup>,  
5 Kerem İlaslan<sup>1</sup>, Ozlem Torun<sup>1</sup>, Fahriye Ceyda Dudak Şeker<sup>1</sup>

6

7 **Affiliation of the authors:**

8 <sup>1</sup> Department of Food Engineering, Faculty of Engineering, Hacettepe University, Beytepe  
9 06800 Ankara, Turkey

10 <sup>2</sup> Food Research Center, Hacettepe University, Beytepe 06800 Ankara, Turkey

11

12

13 **\*Corresponding author:**

14 Prof. Dr. İsmail Hakki Boyacı

15 Hacettepe University

16 Department of Food Engineering

17 Beytepe, 06800 Ankara, TURKEY

18 Phone: +90 312 297 61 46

19 Fax: +90 312 299 21 23

20 e-mail: [ihb@hacettepe.edu.tr](mailto:ihb@hacettepe.edu.tr)

21

22 Raman spectroscopy is a powerful technique for molecular analysis of food samples. A  
23 fingerprint spectrum can be obtained for a target molecule by using Raman technology, as  
24 specific signals are obtained for chemical bonds in the target. In this way, food components,  
25 additives, process and changes during shelf life, adulterations and numerous contaminants  
26 such as microorganisms, chemicals and toxins, can also be determined with or without the  
27 help of chemometric methods. The studies included in this review show that Raman  
28 spectroscopy has great potential for food analyses. In this review, we aimed to bring together  
29 Raman studies on components, contaminants, raw materials, and adulterations of various  
30 food, and attempted to prepare a database of Raman bands obtained from food samples.

31

32

33

34 **Key words:** Raman Spectroscopy, food analysis, food components, contaminants, Raman  
35 bands database

36

## 37 Introduction

38

39 Customers have recently become more concerned about being informed on food quality and,  
40 thus the need for food quality determination methods has increased. Therefore, all steps in  
41 food production such as composition or quality of the products, their origin and how they  
42 have been handled, processed and stored have gained importance. Various types of methods,  
43 including microbial methods, sensory analysis, biochemical and physicochemical methods are  
44 used in food analysis. Chromatographic methods such as high-performance liquid  
45 chromatography (HPLC) and gas chromatography (GC) have become very popular for  
46 separation and identification of food components due to their high reproducibility and low  
47 detection limits.<sup>1</sup> Deoxyribonucleic acid (DNA) based methods, such as Polymerase Chain  
48 Reaction (PCR) techniques, and immunological based methods, such as Enzyme-Linked  
49 Immunosorbent Assay, are also used for detection of specific targets in food samples.  
50 Although these are common methods being used, they cannot meet the demand for *in situ*,  
51 rapid and multiple analysis. Spectrophotometric methods, on the other hand, has a great  
52 advantage over them as it successfully meets those requirements. Spectroscopic methods  
53 which are used to determine different properties of food components is a rapid and easy  
54 method.<sup>2</sup> The spectroscopic methods used for food analysis include Ultra Violet-Visible  
55 Spectroscopy (UV-Vis spectroscopy), Fluorescence Spectroscopy, Raman Spectroscopy and  
56 Infrared Spectroscopy (IR), Circular Dichroism (CD), X-ray Spectroscopy, Nuclear Magnetic  
57 Resonance, Electron Spin Resonance, Dielectric Spectroscopy, and Photoacoustic  
58 Spectroscopy.

59 Raman spectroscopy detects chemical and organic molecule types and their physical  
60 structures by making use of bonds.<sup>2</sup> Photons are scattered when an intense monochromatic  
61 light source -especially a laser beam- irradiates a sample, and as a result of this application,

62 the largest fraction of the scattered light is found to have the same wavelength as the laser  
63 light. This elastic scattering is known as Rayleigh scattering. Far fewer inelastic collisions  
64 occur between the sample and the incident photons. As a result, the wavelengths of scattered  
65 photons change, which is referred to as Raman scattering (Fig.1). If a molecule gains energy  
66 during Raman scattering, the scattered photons will shift to longer wavelength and give  
67 Stokes lines; however, if it loses energy, they may shift to shorter wavelengths and give anti-  
68 Stokes lines, as seen in Fig 1.<sup>3</sup> The quantity of normal vibrations, masses and geometric  
69 arrangements of the atoms in the molecule, as well as the strengths of the chemical bonds  
70 between the atoms, form the vibrational spectrum or *fingerprint* of each molecule. The term  
71 fingerprint is justified by the fact that no two samples or compounds have the same spectrum  
72 in terms of frequency and intensity of peaks and shoulders.<sup>4</sup> Molecules have a large number  
73 of vibrational states, but not all molecules are able to have a Raman spectrum. Being Raman  
74 active is the basic requirement for a molecule to have a Raman spectrum. Raman  
75 spectroscopy can examine molecular vibrations that cause change in their polarizability.<sup>5</sup> The  
76 symmetry of a molecule is also an important requirement for Raman spectra, since symmetric  
77 stretches are more intense in Raman spectra than in Infrared spectra. Functional groups such  
78 as C-X (X=F, Cl, Br or I), C-NO<sub>2</sub>, C-S, S-S, C=C, C≡C, C≡N, etc., show greater  
79 polarizability changes and give strong Raman signals.<sup>5</sup>

80 A Raman spectrum consists of scattering intensity (photons per second) plotted vs.  
81 wavelength (nanometres) or Raman shift (in reciprocal centimetres). Each band in a Raman  
82 spectrum corresponds to a Raman shift occurring due to the incident light energy.<sup>6</sup> These  
83 bands correspond to specific bands of chemical bonds and/or functional groups of the  
84 molecule. By using these specific bands, the fingerprint of a molecule can be obtained with  
85 Raman spectroscopy. In addition, quantitative analyses can also be performed by using

86 Raman spectroscopy since the intensity of the band is linearly proportional to the  
87 concentration of an analyte.<sup>3</sup>

88 Raman spectroscopy has great potential for biochemical analysis. Major advantages of  
89 this technique are its ability to provide information about concentration, structure, and  
90 interaction of biochemical molecules within intact cells and tissues non-destructively. In  
91 addition, it doesn't require homogenization, extraction, the use of dyes or any other labelling  
92 agent,<sup>7</sup> or any pre-treatment of samples; it only requires small portions of samples. Raman  
93 spectroscopy can analyse samples in both liquid and solid phases at ambient temperature and  
94 pressure.<sup>8</sup> Besides, Raman spectroscopy is a potential tool for the assessment of food quality  
95 systems during handling, processing and storage.<sup>9</sup>

96 In this review, we will discuss applications of Raman spectroscopy in food analysis  
97 (Fig. 2). Conventional analysis methods will be taken into consideration under the headings  
98 related to each basic food sample. These headings are listed as Raman Spectroscopy for  
99 detection of food components, microorganisms and chemicals in food, food additives, raw  
100 materials and food adulterations; and relevant studies are presented under each of them. In  
101 addition, vitamins and minerals will be also considered although they found little interest in  
102 food analysis by Raman despite of their major role in nutrition and health. There are several  
103 reviews in literature about usage of Raman Spectroscopy for food analysis focusing on  
104 specific food groups or specific components found in foods.<sup>10-13</sup> This review will provide a  
105 general insight into the Raman analysis of major components and contaminants found in  
106 foods including adulterations. Besides, Raman bands of the important compounds found in  
107 food matrix will be presented in a database, which will be helpful for the user of the Raman  
108 spectroscopy to analyze new spectra obtained from food samples. Although surface-enhanced  
109 Raman Spectroscopy (SERS) is a commonly used method for improving the sensitivity of  
110 Raman Spectroscopy, studies on SERS haven't been included in this review since it requires a

111 specific surface and a Raman active molecule in order to provide enhancement and to obtain  
112 characteristic Raman signals.

113

## 114 **Raman spectroscopy for the detection of food components**

115 Composition of the food samples has great importance due to its substantial effect on quality,  
116 nutritional and economic value, and its contribution to the properties of final product.

117 Environmental factors and applied processing factors could have both positive and negative  
118 effects on food components. Therefore, monitoring these changes in every step of food

119 production process is of great importance. There are many ways to determine these changes in  
120 food components, and for this purpose, there has been an increasing interest in the use of

121 Raman spectroscopy over the past few decades. In this section, an overview is given on the  
122 use of Raman spectroscopy in quantitative and qualitative analysis of food components.

123 Specific Raman bands related to the articles investigated in this section were given in Table  
124 1S, 2S, 3S and 4S for proteins, carbohydrates, lipids and vitamins, respectively.

125

### 126 **Proteins**

127 Raman spectroscopy enables researchers to obtain detailed information on structural  
128 properties of proteins. Studies on food proteins have been conducted for several decades, and

129 they still maintain their importance since proteins are one of the major components of foods  
130 and have important effects on properties of food. Proteins are large polypeptides consisting of

131 hundreds of amino acids; thus, a complex set of overlapping bands forms their Raman spectra.  
132 Additionally, strong Raman scattering of aromatic amino acids and polypeptide chains also

133 contribute to the existence of characteristic bands observed in the Raman spectra.<sup>14</sup>

134 Raman spectroscopy has been used in food protein studies on various topics, but in  
135 particular, investigation of the secondary structure of proteins has been the focus of them. In

136 these studies, amide bands-especially the amide I (1645–1685  $\text{cm}^{-1}$ ) and amide III (1200–  
137 1350  $\text{cm}^{-1}$ ) bands have proven to be the most useful bands to obtain data on the secondary  
138 structures of proteins, which are composed of  $\alpha$ -helices,  $\beta$ -sheets, turns and random coil  
139 structures. Characteristic Raman bands of various amino acid residues have also been used to  
140 acquire information about the microenvironment and conformational changes of the proteins.  
141 For instance, phenylalanine residue has been generally used as an internal standard in most of  
142 the Raman spectroscopic studies<sup>15-17</sup> since it is reported to be insensitive to conformation or  
143 microenvironment.<sup>18</sup> Chi et al. used the advantages of UV-resonance Raman spectroscopy  
144 (UV-RR spectroscopy), such as its ability to selectively examine the secondary structures of  
145 dilute protein and peptide solutions.<sup>19</sup> Chemometric methods were employed to determine the  
146 average amide band resonance Raman spectra of the  $\alpha$ -helix,  $\beta$ -sheet, and unordered  
147 secondary structures of a number of proteins. Similarly, Huang, Balakrishnan, and Spiro used  
148 deep-UV-RR spectroscopy to investigate the secondary structures of proteins.<sup>20</sup> Resonance-  
149 enhanced amide bands and aromatic side chain bands of proteins with varied secondary  
150 structure contents were analysed with least-squares fitting method to establish quantitative  
151 signatures of secondary structure.

152 Several reactions occurring in the food matrix due to application of different processing  
153 techniques could be monitored by Raman spectroscopy. Nonaka, Li-Chan, and Nakai studied  
154 thermal-induced gelation process of whey proteins. Different time and temperature parameters  
155 were applied to  $\alpha$ -lactoglobulin and  $\beta$ -lactoglobulin proteins, and changes in their Raman  
156 spectra were followed.<sup>21</sup> In another study, Raman spectroscopy was used to investigate the  
157 interaction of lysozyme,  $\alpha$ -lactoglobulin and  $\beta$ -lactoglobulin before and after the completion  
158 of gelation process.<sup>22</sup> Rheological changes and the interactions of egg albumen and whey  
159 protein during the gelation process were tracked with FT-Raman spectroscopy using  
160 phenylalanine (1004  $\text{cm}^{-1}$ ) as an internal standard. Differences in the gel structures were

161 evaluated by monitoring CH ( $1350\text{ cm}^{-1}$ ) and CH<sub>2</sub> ( $1450\text{ cm}^{-1}$ ) bending vibrations. As a result,  
162 an increment was observed for the Raman intensity of  $\beta$ -sheet structures in the amide III  
163 region, while the intensities decreased for helical structures.<sup>17</sup> Sánchez-González et al. used  
164 FT-Raman to examine the structural changes in proteins and water during gelation of fish  
165 surimi. Amide bands and amino acid residue bands were monitored to detect the changes.<sup>23</sup>  
166 The changes in chemical structures occurring due to heat treated gelatinization of myofibrillar  
167 proteins contribute to the quality of meat products and to improve their production techniques.  
168 Hence, conformational changes in peptid structures of meat, which is highly rich in protein,  
169 were tracked by using Raman spectroscopy. It was found that owing to the impact of heat,  
170 changes in amide I ( $1600\text{-}1700\text{ cm}^{-1}$ ) and amide III ( $1200\text{-}1300\text{ cm}^{-1}$ ) regions reduces the  $\alpha$ -  
171 heliks content in protein structure, while it increases  $\beta$ -sheets,  $\beta$ -turns and random coil  
172 content.<sup>24</sup> In another study, whether endpoint temperature (EPT) was reached for cooked meat  
173 and meat products was checked by using Raman Spectroscopy with chemometric analysis. It  
174 was found that seconder structure of meat proteins were changed with heat treatment as in the  
175 previous study.<sup>25</sup> Lim et. al., studied gelation of phenol extracted protein fractions from non-  
176 acclimated (NA) and cold-acclimated (CA) winter rye leaf tissue after repeated freeze-thaw  
177 treatments. Changes in the protein secondary structure caused by the freeze-thaw cycles were  
178 monitored by using Raman microscopy. Gelling and non-gelling components as well as  
179 protein extracts were individually analyzed with Raman measurements. Similarity between  
180 NA and CA samples was explained with their similar structural conformations, which were  
181 stabilized by similar protein-protein interactions, while dissimilarities were mainly assigned to  
182 the covalent bonds altered by freeze-thaw treatments.<sup>26</sup> Lactate dehydrogenase was chosen as  
183 a model protein to evaluate the potential of Raman spectroscopy for discriminating native like  
184 and non-native states of protein in freeze-dried formulations. PCA and PLS-LDA methods  
185 were applied to collected Raman data for discrimination studies. Different prediction models

186 were developed using different spectral regions and their combinations. C-N stretch, NH<sub>3</sub>  
187 deformation, amide III, and mainly C-H<sub>n</sub> non-stretching with possible participations of C-N  
188 and C-C stretching were considered to have the maximum contribution to the success of  
189 discrimination.<sup>27</sup>

190 Deamidation of proteins is another process which can be easily followed by using  
191 Raman spectroscopy. Wong et al. used soy and whey protein isolates and spray-dried egg  
192 white powder to analyze the extent of deamidation in food proteins. Conformational changes  
193 of the protein structures were examined using Raman spectroscopy. Characteristic band,  
194 which was assigned to the stretching of the C=O bond of glutamate or aspartate, was used as  
195 the marker band for deamidation.<sup>28</sup> In another work, the enzymatic hydrolysis of wheat gluten  
196 substrates, which were acid-deamidated by using three different acids were determined with  
197 Raman spectroscopy. The same degree of deamidation with the same heat treatment  
198 conditions was applied to all substrates. Raman spectroscopic analyses of microenvironments  
199 belonging to Cys, Trp, Tyr and His amino acids showed a positive relation with their  
200 susceptibilities to enzymatic hydrolysis.<sup>16</sup>

201 Kang et al. used Raman spectroscopy to evaluate the effects of salt content and also  
202 chopping and beating processes on the structural components of pork frankfurters. In the case  
203 of increased salt content, a decrease was observed for C-H stretching, CH<sub>2</sub> and CH<sub>3</sub> bending  
204 vibrations, while no changes were witnessed for secondary structures, namely tryptophan,  
205 tyrosine residues,  $\beta$ -sheet and  $\alpha$ -helix. Beating process was resulted with an increase in  $\beta$ -  
206 sheet, a decrease in  $\alpha$ -helix content and a decrease in C-H stretching, CH<sub>2</sub> and CH<sub>3</sub> bending  
207 vibrations. The adequacy of Raman spectroscopy as the experimental technique to follow the  
208 changes (appearing and disappearing of compounds) in composition during the beating  
209 process was demonstrated in this study.<sup>29</sup>

210 The interactions of proteins with other food components are another topic of interest  
211 commonly dealt with in using studies Raman spectroscopy. Shao et al, for instance, used  
212 Raman Spectroscopy to examine the emulsion created by adding lipid to meat. They followed  
213 the changes occurring in protein structures due to addition of different lipids to meat and heat  
214 treatment. They found that there wasn't a considerable change in the secondary structures of  
215 proteins in emulsion spectra obtained by mixing three different kinds of lipids without any  
216 heat treatment. With the application of heat treatment, however, it was seen that changes  
217 occurred in the bands ( $1153\text{ cm}^{-1}$ ) demonstrating amide I ( $1654\text{ cm}^{-1}$ ), amide II ( $1517\text{ cm}^{-1}$ ),  
218 amide III ( $1300\text{ cm}^{-1}$ ) and C-N stretching vibration, and that formation of  $\beta$ -sheet increased.  
219 In this way, the researchers put forward the idea that with Raman spectroscopy,  
220 protein/lipid/water interactions could be examined and information could be obtained  
221 directly.<sup>30</sup> Meng et al., however, examined the protein-lipid interaction with Raman  
222 microscopy by using bovine serum albumin/oil. Different spectra were obtained by extracting  
223 the spectrum of mineral or corn oil from that of the bovine serum albumine (BSA)/oil  
224 interface in order to determine the contributions of different functional groups to the protein-  
225 lipid interactions.<sup>31</sup> In the study of Sivam et. al., Raman and FT-IR spectroscopy were used as  
226 complementary methods to explore the conformational changes in wheat proteins and  
227 polysaccharides due to their interactions with fruit polyphenols and pectin. Amide bands, in  
228 particular, were examined to comprehend the interactions between additives and gluten  
229 proteins by following changes in the secondary structures of the proteins.<sup>32</sup> In the study of  
230 Ferrer et. al., gluten protein was chemically modified with an emulsifier, namely sodium  
231 stearyl lactylate (SSL), and the effect of the modification on the secondary and tertiary  
232 structures of this protein was analysed with FT-Raman spectroscopy. A significant increase  
233 was observed in the intensity of amide I band, which is attributed to a more ordered structure.  
234 Conformational variations of disulfide bounds and the variations of the intensity rate of the

235 tyrosine doublet bands, tryptophan and C-H stretching band were also explained by formation  
236 of a more ordered structure.<sup>15</sup> In the subsequent study of the same group, Gomez et. al.  
237 reported a more detailed research investigating the conformational changes in the presence of  
238 another emulsifier, namely diacetyl tartaric acid esters of monoglycerides: DATEM. A  
239 comparison was also made on the differences in the gluten structures occurring in the  
240 presence of DATEM and SSL, respectively. Differences on Raman spectra were mainly  
241 assigned to the distinct chemical structures of these emulsifiers which specify their type of  
242 interactions with gluten proteins.<sup>33</sup> Perisic et. al. used the combinations of vibrational  
243 spectroscopic techniques, namely NIR spectroscopy and FT-IR, NIR and Raman  
244 microspectroscopy to study the effects of different salts on the hydration properties of  
245 structural proteins. Interactions between salt cations and aromatic amino acid residues were  
246 investigated, and their effect on the final structure of proteins was emphasized. Effect of salt  
247 concentration on the protein structures were mainly monitored with tyrosine bands which  
248 were in a positive correlation with hydrogenated N-H groups.<sup>34</sup>

249

## 250 **Carbohydrates**

251 Structural characterization of carbohydrates is of great importance since they form the widest  
252 class of organic compounds. Mono-, di-, oligo- and polysaccharides show characteristic  
253 Raman bands by which carbohydrates can be easily determined and quantified. Presence of  
254 large number of atoms in the repeat unit and absence of a well-defined entity increased the  
255 importance of accurate assignement of vibrational modes in the structural analysis of  
256 carbohydrates by using Raman spectroscopy.<sup>35</sup> For instance, the amylose contents of corn and  
257 cassava starch samples were quantified using FT-Raman spectroscopy coupled with PCA and  
258 PLS regression methods. Characteristic band at  $480\text{ cm}^{-1}$  was assigned to the ring vibration of  
259 starches and used to identify the presence of starch and to distinguish between corn and

260 cassava starch samples.<sup>36</sup> Delfino et al. quantified the glucose contents in commercial sports  
261 drinks by using micro-Raman and interval Partial Least Square regression (iPLS). Fingerprint  
262 bands of glucose, fructose and sucrose were obtained in the spectral region between 600  
263 and 1600  $\text{cm}^{-1}$ .<sup>37</sup> In a recent study reported by our research group, Ilaşlan et. al. used Raman  
264 spectroscopy to quantify glucose, fructose and sucrose contents of commercial soft drinks.  
265 Additives in the content of soft drinks were also characterized by their bands, which were  
266 assigned to the presence of aroma compounds and citric acid in the composition. The  
267 calibration curves were obtained for each component by applying PLS regression on Raman  
268 data, and validation studies were carried out using HPLC.<sup>38</sup>

269 Raman spectroscopy was also used for the detailed investigation of structural  
270 components of the food samples. In the study of Roman et al., the components of wild carrot  
271 root, such as starch, pectin, cellulose, lignin, and even bioactive polyacetylenes were  
272 measured in situ and without any sample preparation. They also showed tissue-specific  
273 accumulations of the components using a Raman mapping technique.<sup>39</sup> In a similar study,  
274 components of wheat and barley grain were investigated using Raman microscopy. The  
275 Raman spectra of the most important substances such as proteins, carbohydrates  
276 (arabinoxylan,  $\beta$ -glucan and starch) and phytic acid were included in the compositions of  
277 barley, and wheat cells were measured. Wheat proteins were monitored by using the  
278 characteristic bands of gluten located around 1449 and 1659  $\text{cm}^{-1}$ , which was attributed to the  
279  $\text{CH}_2$  bending mode of amino acids and  $\text{C}=\text{O}$  stretching mode of amides, respectively.  
280 Polysaccharides, namely arabinoxylan,  $\beta$ -glucan and starch gave similar Raman spectra.  
281 Distinct bands at 1095 and 1120  $\text{cm}^{-1}$  assigned to the COC stretching vibrations of glycosidic  
282 bonds showed the most evident similarity between these spectra. Starch was separated from  
283 the other polysaccharides by its characteristic bands at 480 and 901  $\text{cm}^{-1}$  (skeletal vibrations  
284 of the glucopyranose ring), and phytic acid gave relatively weak Raman scattering with a

285 characteristic band at  $3420\text{ cm}^{-1}$ , (stretching of OH group). Raman imaging was also  
286 performed to analyze the distribution of these components in the cereal grain structure.<sup>40</sup>

287 Application of Raman spectroscopy makes it possible to determine the sources of  
288 carbohydrates and extract minor differences between very similar structures. Scudiero and  
289 Morris used Raman spectroscopy to identify the differences between soft and hard wheat flour  
290 samples. Relative intensity ratios of the bands between  $400\text{-}600\text{ cm}^{-1}$  and  $1020\text{-}1650\text{ cm}^{-1}$   
291 corresponding to the arabino-to-xylan substitution and phenolic acid contents were used to  
292 differentiate the samples.<sup>41</sup> Wellner et al. compared the composition and physical structure of  
293 starch granules found in wild type and mutant maize kernels by using a Raman imaging  
294 technique.<sup>42</sup> Similar characteristic bands of carbohydrates and protein structures, specifically  
295 amide I bands were observed for both wild type and mutant samples. However, differences  
296 originating from the variations in the ratio of branched residues to linear residues were  
297 monitored by following the characteristic band at  $942\text{ cm}^{-1}$ , which was reported as being  
298 sensitive to the level of branching in starch polysaccharide. Another characteristic band at  $865$   
299  $\text{cm}^{-1}$  was used to monitor the crystalline structure of starch granules.<sup>43</sup> Compositional and  
300 structural properties of  $\beta$ -glucan in barley and oat samples were investigated with FT-Raman  
301 spectroscopy. PCA and PLS regression were used for multivariate data analysis of collected  
302 Raman data, especially in the spectral region between  $800$  and  $1800\text{ cm}^{-1}$ . PLS regression  
303 prediction models successfully determining the  $\beta$ -glucan and starch contents of the samples  
304 were created. Clusters of cellulose, curdlan and cellulose-curdlan blends were located in the  
305 PCA score plot depending on the variation in their  $\beta$ -glucan structure.<sup>44</sup>

306 The effects of food processing on carbohydrates, one of which is starch modification,  
307 have also been analysed with Raman spectroscopy. Chong et al. determined the degree of  
308 maleate substitution in maleinated starches depending on the emergence of new bands, which  
309 were likely due to nominal C=O stretch, C=C stretch, and O-H stretch vibrational modes.<sup>45</sup>

310 Another modification of starch was carried out with octenyl succinate. This modification  
311 treatment was monitored using Raman microscopy entegrated with AFM.<sup>46</sup> The use of Raman  
312 spectroscopy for quality control of modified starches in the food industry was demonstrated  
313 by Dupuy and Laureyns. They identified the modified starches according to their origin and  
314 type of modification. Although an overall similarity was observed for different starch  
315 samples, disappearance of the doublet at  $600\text{ cm}^{-1}$  was observed for pregelatinized samples.  
316 Similarly, waxy samples were monitored by their characteristic bands at 480, 870, 950 and  
317  $1468\text{ cm}^{-1}$ , which were assigned to skeletal mode, the CH and  $\text{CH}_2$  deformation, the skeletal  
318 mode involving  $\alpha$  (1–4) linkage and the  $\text{CH}_2$  deformation, respectively. They also compared  
319 the efficiency of the chemometric methods PCA and PLS in order to group the samples  
320 according to the applied modification type and draw the conclusion that PLS is more effective  
321 than PCA.<sup>47</sup> Passauer et al. studied the degrees of substitution (DS) of starch phosphates by  
322 using the characteristic band of C-O-P stretching vibration at about  $975\text{ cm}^{-1}$ .<sup>48</sup> Volkert et al.  
323 also determined the DS values of different substituted starch acetates by using a combination  
324 of FT-Raman spectroscopy and chemometrics. They found the best congruence between  
325 determined and calculated DS values by calculating the first derivatives of the Raman  
326 spectra.<sup>49</sup> In another study, DS values for cationic quaternary ammonium starches were  
327 determined using the characteristic band of trimethyl ammonium substituent about  $761\text{ cm}^{-1}$ .<sup>50</sup>  
328 Similarly, the DS values for carboxymethylated non-starch polysaccharides including  
329 cellulose, guar gum, locust bean gum and xanthan gum were determined with Raman  
330 spectroscopy and a colorimetric method. The characteristic band at  $1607\text{ cm}^{-1}$  was chosen to  
331 be the marker of carboxymethylation which originates from C=O carbonyl stretching  
332 vibration. The intensity ratios of the marker bands to that of an internal standard band  
333 corresponding to the skeletal configuration and linkages ( $850\text{--}950\text{ cm}^{-1}$ ) were used to  
334 establish a calibration between spectroscopic and colorimetric DS values.<sup>51</sup>

335 In another study, the technical starch hydrolysis process was monitored with FT-  
336 Raman.<sup>52</sup> Gelatinization, liquefaction, saccharification and retrogradation processes were  
337 evaluated within the context of the relevant study. The intensity of the bands at 1633 and 3213  
338  $\text{cm}^{-1}$  increased during the gelatinization process, while the others decreased. Liquefaction was  
339 characterized by the disappearance of the bands at 735  $\text{cm}^{-1}$  and 480  $\text{cm}^{-1}$ . Changes in  
340 saccharification at bands in 910–935  $\text{cm}^{-1}$  region and at 1127  $\text{cm}^{-1}$  were also monitored.<sup>53,54</sup>

341 Mutungi et al. demonstrated the utility of the FT-Raman method for rapidly determining  
342 starch crystallinity, which is important for food production and storage. In this method, a band  
343 assigned to symmetric C(1)-O-C(5) stretching of the  $\alpha$ -D-glucose ring was used as an internal  
344 standard to normalize the spectra. As a result, a strong linear correlation was found between  
345 crystallinity and the integrated area of the skeletal mode Raman band.<sup>55</sup> Similarly, in the study  
346 of Islam and Langrish, Raman spectroscopy was used to investigate the formation of lactose  
347 anomers and degree of lactose crystallization during spray drying. The characteristic bands in  
348 the Raman spectra indicated the presence of different lactose anomeric and crystalline forms.  
349 These bands at 1100 and 350  $\text{cm}^{-1}$  were assigned to the stretching and bending vibrations of  
350 the C-O-C grouping of  $\alpha$ - and  $\beta$ -lactose structures. Spectral region between 1200 and 1500  
351  $\text{cm}^{-1}$  was used to characterize the presence of an amorphous polymorph in the lactose  
352 samples.<sup>56</sup> In another study on crystallinity, Raman spectroscopy was used to determine the  
353 viscoelastic properties of modified cellulose, which is a significant substance in food  
354 industry. Akinosho et. al. investigated the effect of methyl and hydroxypropyl groups on gel  
355 properties of hydroxypropyl methylcellulose (HPMC). Subsequent to the analysis of collected  
356 Raman data, usability of the hydroxypropyl groups as an indicator of the crystalline structure  
357 of HPMC was reported. Crystallinity was also monitored by following the significant  
358 broadening, which is generally assigned to the decrease in crystallinity in the spectral region  
359 between 1540–1660  $\text{cm}^{-1}$ .<sup>57</sup>

360 Kizil and Irudayaraj evaluated the potential of Raman spectroscopy to follow the  
361 chemical changes induced by the application of gamma-irradiation to food samples. Fructose  
362 and honey samples were analysed using FT-Raman spectroscopy and canonical discriminant  
363 analysis was applied to the collected data. Monitoring the CH stretch region between 2800  
364 and 3000  $\text{cm}^{-1}$ , they classified honey samples according to applied irradiation dose. Using  
365 spectral regions below 700  $\text{cm}^{-1}$  and between 800 and 1500  $\text{cm}^{-1}$ , changes in the ring and  
366 conformational structure of the fructose induced by irradiation were identified.<sup>58</sup>

367 The mechanism of thermal radical generation in cereal starches with different amylose  
368 contents was analysed by using a Raman microspectrometer. Effects of high temperature on  
369 the structure of polysaccharide molecules were tracked from the collected Raman spectra.  
370 Due to the decomposition of polysaccharide chains by the cleavages of the glycosidic bonds,  
371 the highest amount of decrease was observed for the bands at  $\nu_a$  (1150  $\text{cm}^{-1}$ ) and  $\nu_s$  (944  
372  $\text{cm}^{-1}$ ) of C-O-C.<sup>59</sup> Different from the previous one, in this study, how freezing treatment  
373 affects the structure of wheat bread dough was examined with Raman spectroscopy. The  
374 distribution of ice free water, starch, gluten and yeast in the frozen dough in the structure was  
375 determined by examining the Raman bands of each of these components, and the  
376 microstructure of the dough was determined by making use of images. In this way,  
377 researchers stated that the causes of the decrease in quality can be found in the frozen baked  
378 goods.<sup>60</sup>

379

### 380 **Lipids**

381 Lipids are one of the three major food components, but they have been reported as the most  
382 complex molecular structures to be analysed. Raman spectroscopy has been widely used for  
383 determining different properties of lipids. For instance, Sadeghijorabchi et al. put forward a  
384 procedure that determines the total level of unsaturation in oils and fats by using FT-Raman

385 spectroscopy.<sup>61</sup> Similarly, Silveira et al. quantified unsaturated fats in fat-containing foods.  
386 Raman spectra of edible oils, margarine, mayonnaise, hydrogenated fat, and butter were  
387 obtained with a near-infrared Raman spectrometer by making use of this non-destructive  
388 quantification method. Spectral regions of 1750, 1660, 1440, 1300, and 1260  $\text{cm}^{-1}$  were used  
389 to establish a correlation between Raman intensities and the total and unsaturated fat contents  
390 of analyzed samples.<sup>62</sup> El-Abbasy et al. quantified the fat content in liquid homogenized milk  
391 by using VIS-Raman spectroscopy. Protein and carbohydrate content of milk samples didn't  
392 made a significant influence on the Raman intensities, so the variations were directly  
393 attributed to the fat contents of the samples. Characteristic bands were mostly assigned to the  
394 fatty acids and monitored at bands in 1650  $\text{cm}^{-1}$  (C=C *cis* double bond stretching of  
395 RHC=CHR), 1440  $\text{cm}^{-1}$  (C-H scissoring of  $-\text{CH}_2$ ), 1265  $\text{cm}^{-1}$  (C-H bending at the *cis* double  
396 bond in R-HC=CH-R), 1300  $\text{cm}^{-1}$  (C-H twisting of the  $\text{CH}_2$  group), and 1747  $\text{cm}^{-1}$  (C=O  
397 stretching of RC=OOR).<sup>63</sup> McGoverin et al. used Raman spectroscopy to quantify milk  
398 powder constituents, namely protein and fat in skim and whole milk samples. The overlapped  
399 bands seen in Raman spectra are considered to be caused by lactose, milk proteins and milk  
400 fats. The characteristic band represented by lower wavenumber 1745  $\text{cm}^{-1}$  C=O modes were  
401 assigned to milk fat, while the phenylalanine ring breathing band at 1005  $\text{cm}^{-1}$  was accepted  
402 as the indicative of protein. A low broad peak above 3300  $\text{cm}^{-1}$  was reported to be consistent  
403 with N-H and O-H modes of protein and lactose.<sup>64</sup> A combination of Raman spectroscopy  
404 with chemometric methods enabled researchers to establish predictive models for these  
405 constituents by using abovementioned characteristic bands. This combination has also been  
406 used to predict the abundance of fatty acids in clarified butterfat,<sup>65</sup> and to discriminate and  
407 classify different oils and fats.<sup>66-68</sup> Marquardt et. al. used Raman spectroscopy to obtain  
408 quantitative data on carotenoid, collagen and fat contents of the fish muscle samples. Fat  
409 content was characterized by the bands at 657, 1440, 1301 ( $\text{CH}_2$  in phase twist), 1267(C-H

410 symmetric rock (*cis*), 1076 (C-C-C stretch) and 1064  $\text{cm}^{-1}$  (C-C-C stretch). Carotenoids were  
411 monitored at primary bands (1159 and 1518  $\text{cm}^{-1}$ ), and the intensity of the bands at 857  
412 (proline) and 940  $\text{cm}^{-1}$  (C-C stretch of peptide backbone) which were assigned to the  
413 presence of collagen was found to be relatively weak.<sup>7</sup>

414 Lipid oxidation, one of the most important quality indicators in foods, has been  
415 investigated with Raman spectroscopy. Muik et al. examined the chemical changes that  
416 occurred during lipid oxidation in edible oils.<sup>69</sup> Kathirvel et al. monitored the progression of  
417 lipid oxidation in mechanically separated turkey by monitoring the oxidative bleaching of  $\beta$ -  
418 carotene using Raman spectroscopy. Three characteristic Raman bands at 1008  $\text{cm}^{-1}$  from the  
419 C-CH<sub>3</sub> rocking, at 1160  $\text{cm}^{-1}$  from the C-C stretching and at 1524  $\text{cm}^{-1}$  from the C=C  
420 stretching were observed for  $\beta$ -carotene molecule, while the last one was used to monitor its  
421 concentration.<sup>70</sup> Guzman et al. determined the oxidation status of olive oil through a  
422 combination of low-resolution Raman spectroscopy and PLS analysis. In order to monitor  
423 olive oil oxidation, characteristic Raman bands at 1267  $\text{cm}^{-1}$ , 1302  $\text{cm}^{-1}$ , 1442  $\text{cm}^{-1}$  1655  
424  $\text{cm}^{-1}$ , and 1747  $\text{cm}^{-1}$  (corresponding to symmetric rock double bond in *cis* =CH, in-phase  
425 twist methylene, methylene scissoring mode of CH<sub>2</sub>, *cis* double bond stretching (C=C), and  
426 ester stretching (C=O), respectively) were detected in the region below 1800  $\text{cm}^{-1}$ .<sup>71</sup> In  
427 addition to these applications, it is also possible to show the effects of storage conditions on  
428 lipids or lipid containing foods. Sanchez-Alonso et al. used FT-Raman spectroscopy to  
429 monitor the lipid oxidation of hake fillets during frozen storage. C-C stretching vibration at  
430 1658  $\text{cm}^{-1}$  was reported as the only characteristic Raman band related to the lipid oxidation.<sup>72</sup>

431 A study was carried out using linoleic acid, which is a very important fatty acid in  
432 human diet. In this study, linoleic acid was treated with high pressure. Linoleic acid's phase  
433 transition and conformational changes with high pressure were observed in real-time by using  
434 Raman spectroscopy. Significant conformational changes were observed at 0.07-0.12 GPa and

435 0.31-0.53 GPa. With the increase in pressure, some Raman bands disappeared, while some of  
436 them appeared. The researchers believe that knowledge about these chemical and physical  
437 changes will make the major contribution to food preservation technology.<sup>73</sup> Another essential  
438 oil produced out of *Lamiaceae* plant displaying different chemical profiles according to their  
439 genomic properties has a biological activity of great importance. In the light of these  
440 informations, chemical structures of the essential oils were determined using dispersive  
441 Raman spectroscopy and FT-IR. Chemotyping was based on characteristic bands of thymol  
442 ( $740\text{ cm}^{-1}$  ring vibration) and carvacrol ( $760\text{ cm}^{-1}$ ), and the results were confirmed by using  
443 GC.<sup>74</sup>

444 Researchers used Raman spectroscopy to follow the changes in carotenoid structure of  
445 extra virgin olive oil with heat treatment, which was applied by using microwave and  
446 conventional heating processes. It was shown that conventional heat treatment caused more  
447 rapid degradation of carotenoid bands at  $1008\text{ cm}^{-1}$  (C-CH<sub>3</sub> bend),  $1150\text{ cm}^{-1}$  (C-C stretch),  
448 and  $1525\text{ cm}^{-1}$  (C=C stretch). In addition, the researchers found that high heat treatment  
449 resulted in whole degradation of carotenoids and that application time plays a more important  
450 role in the degradation compared to high temperature. They determined that heat treatment  
451 with microwave during oil refinement affects the oil quality less than the conventional heat  
452 treatment since the desired temperature was achieved by microwave more quickly than  
453 conventional heating.<sup>75</sup>

454

#### 455 **Vitamins**

456 A variety of analytical procedures have been used for vitamin analysis in food samples. Lack  
457 of specificity and matrix effect were reported as the main disadvantages of these procedures. On  
458 the other hand, Raman spectroscopy has gained an increasing importance due to its high  
459 precision and good signal-to-noise rate for vitamin analysis.<sup>76</sup>

460 Investigation of vitamins with Raman spectroscopy began in the 1970s. Main goals of  
461 these early studies were to characterize the isomeric forms<sup>77</sup> and obtain the characteristic  
462 Raman spectra of vitamins.<sup>78</sup> Rimai et al. acquired the Raman spectra of retinals (*trans*, *9-cis*,  
463 *13-cis*), retinols (*trans*, *13-cis*), and *trans*-retinoic acid in octanol solution and reported the  
464 possibility of characterizing the terminal group on vitamin A type molecules and isomers by  
465 their characteristic bands at around 1580–1590 cm<sup>-1</sup> and 1100–1400 cm<sup>-1</sup>.<sup>77</sup> Similarly, Tsai and  
466 Morris researched the effect of pH and other water soluble vitamins on Raman intensity of  
467 Vitamin B12 by using cyanocobalamin as a model chemical. A strong Raman band at 1504  
468 cm<sup>-1</sup> corresponding to the ring stretching vibration of molecule was followed.<sup>79</sup> Also,  
469 Cimpoiu et al. coupled high performance thin layer chromatography (HPTLC) with Raman  
470 spectrometry in order to obtain a suitable method for identification of eight hydrophilic  
471 vitamins, i.e., B1-thiamin, B2-riboflavin, B3-nicotinic acid, B5-panothenic acid, B6-  
472 pyridoxine, B9-folic acid, B12-cyanocobalamin, and C-ascorbic acid in different samples. In  
473 this study, a successful separation was achieved by HPTLC, and vitamins were easily  
474 characterized by Raman spectroscopy.<sup>80</sup>

475 The use of Raman microscopy also made it possible to determine and localize  
476 vitamins in biological samples. Kim and Carey used riboflavin to differentiate free vitamins  
477 and vitamins bound to vitamin binding proteins at micro molar concentrations.<sup>81</sup> In another  
478 study, Beattie et. al., used Raman spectroscopy to identify  $\alpha$ -tocopherol, which is known to be  
479 the predominant form of vitamin E in biological samples.<sup>82</sup>

480 Additionally, chemometric techniques were used in order to quantify vitamins in  
481 powdered mixtures and solutions. Spectral regions between 2800-3000 cm<sup>-1</sup> and 800-1750  
482 cm<sup>-1</sup> were used for the PLS models due to their high correlation with Vitamin C  
483 concentrations. A detailed chemical assignment was given in the relevant study.<sup>83</sup>

484

## 485 **Raman spectroscopy for microorganism and virus detection**

486 There are several analytical methods to determine the presence of microorganisms and  
487 viruses. Although traditional microbiological plate count methods such as PCR, and  
488 immunological and serological methods have been frequently used for this purpose, Raman  
489 spectroscopy has gained increasing attention due to its abovementioned advantages such as  
490 high sensitivity, reliability and non-destructiveness.<sup>84</sup> In addition to microorganisms that grow  
491 in food, Hepatitis A and Norwalk viruses, Poliovirus, Astrovirus, Enteric adenovirus,  
492 parvovirus and rotaviruses have also been found in foods as contaminants.<sup>84, 85</sup> Specific  
493 Raman bands for microorganism and virus detection were given in Table 5S.

494

### 495 **Microorganisms**

496 Raman and its derivatives, such as UV-RR, FT-Raman, Micro-Raman and Confocal Raman  
497 can be used to determine the presence of microorganisms. By carefully selecting which  
498 Raman method to use, taking advantage of neural networks, and utilizing chemometric  
499 methods to make qualitative distinctions between spectra; it is possible to identify and  
500 differentiate microorganisms.<sup>86, 87</sup>

501 *Bacillus* and *Brevibacillus* species are spore-forming bacteria. *Bacillus* species, in  
502 particular, is pathogenic and causes serious food poisoning incidences; they can also be used  
503 as a biological weapon. Passage from the spore to the vegetative forms of these bacteria, and  
504 determining the effects of manganese dipicolinate and calcium dipicolinate upon spore  
505 formation, were monitored with micro-Raman spectroscopy.<sup>88</sup> In a study made on spore-  
506 forming *Clostridium* cultures, single-cell spectra were collected using confocal Raman  
507 microscopy. Although the morphological structures of the cells were similar, significant  
508 spectral differences were observed between them and their contents depending on age and

509 spore production. As a result, chemical differences between the cells were easily identified by  
510 Raman microscopy.<sup>52</sup>

511 In another study with confocal Raman microscopy, a group of pathogenic  
512 microorganisms (*Enterococci* and *Staphylococci*) was classified. Raman measurements were  
513 taken from different regions of a microcolony of each culture and processed with  
514 chemometric methods. When dendrograms obtained with Hierarchical Cluster Analysis  
515 (HCA) were analysed, two arms were observed, one of which belongs to *Enterococci* and the  
516 other to *Staphylococci*.<sup>89</sup> Specific strains of *Staphylococcus* were identified with a micro-  
517 Raman system. With this methodology, it was possible to determine chemotaxonomic  
518 classification for a single cell and bulk cultures. HCA and Support Vector Machine (SVM)  
519 were used as statistical methods. In one of the analyses, all of the bacteria were incubated  
520 under the same conditions (medium type, incubation temperature and time), and their Raman  
521 spectra were taken. Then, the effect of changes in culture media, incubation temperatures and  
522 times were also analyzed.<sup>90</sup> Another research carried out with *Bacillus* and *Brevibacillus*  
523 species covered identification and differentiation of these bacteria with a UV-RR technique.  
524 The researchers reaffirmed the accuracy of their results with analyses of 16S rDNA of the  
525 bacteria. They stated that genotypic and phenotypic differences between microorganisms  
526 could be detected by using characteristic Raman bands obtained from cellular components  
527 such as aromatic amino acids and UV adsorption-capable nucleic acids. The spectra were  
528 obtained at a wavelength of 244 nm, and subjected to multivariate statistical methods.<sup>91</sup> By  
529 using FT-Raman system, Yang and Irudayaraj separated six different microorganisms (*S.*  
530 *cerevisiae*, *Fusarium verticillioides*, *Bacillus cereus*, *Aspergillus niger*, *Escherichia coli*, *L.*  
531 *casei*) from each other as well as different strains belonging to the same species. They  
532 reported differences due to cell structures within a ‘fingerprint’ range of 600-1800 cm<sup>-1</sup> for  
533 the microorganisms. PCA and CVA were used to characterize these microorganisms.<sup>87</sup> In

534 another study by Maquelin et al., FT-IR and FT-Raman spectra were conducted on dehydrated  
535 *Enterococcus faecalis*. C-H stretching bands belonging to (CH<sub>3</sub>, CH<sub>2</sub>, and CH) functional  
536 groups were observed in the 2700–3000 cm<sup>-1</sup> region, and the deformation band of the C-H  
537 bond at 1450 cm<sup>-1</sup> was also present. Protein amide I and amide II bonds and vibrations of  
538 bases in RNA/DNA were also detected.<sup>92</sup> Colonies of *Micrococcus luteus* (*M. luteus*),  
539 *Bacillus subtilis* (*B. subtilis*), *Pseudomonas fluorescens* (*P. fluorescens*), *Rhodotorula*  
540 *mucilaginosa* (*R. mucilaginosa*), and *Bacillus sphaericus* bacteria were analysed with FT-  
541 Raman. It was found that the spectra of *M. luteus*, *B. subtilis* and *P. fluorescens* had  
542 completely different spectra from each other at a wavelength of 785 nm incident light. As a  
543 result of stimulation with light at 633 nm, distinct templates were obtained from cells  
544 belonging to the pigmented bacteria *M. luteus* and *R. mucilaginosa*.<sup>86</sup> The previously  
545 mentioned group also separated twenty different *Micrococcus*, *Bacillus*, *E. coli* and  
546 *Staphylococcus* strains using micro-Raman spectroscopy coupled with SVM as chemometric  
547 analysis.<sup>90</sup> Raman spectroscopy coupled with different chemometric methods was also used  
548 for the identification of *Legionella*, *Klebsiella*, *Micrococcus*, *Bacillus*, *E. coli*, *Pseudomonas*,  
549 *Staphylococcus*, *Listeria*, *Yersinia* and *Salmonella* species.<sup>93-97</sup>

550 Micro-Raman spectroscopy was also used to distinguish different types of *Lactarius*  
551 mold by using chemometric methods. Lipid and amylopectin were monitored with Raman  
552 spectroscopy since these are characteristic compounds for amyloid reactions of *Lactarius*  
553 spores. *Lactarius* mold is of great importance in ecological and economic sense and popular  
554 in many regions of the world owing to its being edible.<sup>98</sup> Micro-Raman spectroscopy has also  
555 been used to investigate the spatial distribution and composition of lipid vesicles inside intact  
556 hyphae of *Mortierella* species. Differences in the degree of unsaturation and the effect of  
557 growth conditions on lipid composition were determined for *Mortierella alpina* and  
558 *Mortierella elongata* species.<sup>99</sup>

559

560 **Viruses**

561 There have been many studies reporting the use of Raman spectroscopy for structural  
562 characterization of viruses. For instance, a number of studies have been conducted using  
563 structural information obtained out of Raman spectroscopy to develop antiviral drugs.<sup>100-103</sup> In  
564 one of these studies, the formation mechanism of the icosahedral capsid of P22 phage, which  
565 is effective against *Salmonella typhimurium*, was tracked using a Raman microdialysis flow  
566 cell. After preparation of the procapsid, empty shell, and scaffolding protein of the phage, all  
567 the components were placed in the Raman microdialysis flow cell system and their Raman  
568 signals were collected. The results were verified with Sodium Dodecyl Sulfate-  
569 Polyacrylamide Gel Electrophoresis (SDS-PAGE) and the CD spectroscopy. In accordance  
570 with their conclusions, researchers have managed to develop models for the transformation of  
571 procapsid into capsid, and procapsid assembly.<sup>102</sup> UV-Raman has been used to investigate the  
572 protein structure of another phage. Raman spectra of the phage were obtained by excitation at  
573 four different wavelengths (257, 244, 238 and 229 nm). As a result of excitation at 257 nm,  
574 signals of the bases that build the genome were obtained, and characteristic Raman bands  
575 corresponding to the amino acids of the coat protein were attained as a result of excitation at  
576 229 nm.<sup>103, 104</sup> Another research group has benefited from Raman optical activity (ROA) for  
577 the structural characterization of nucleic acids, viruses and proteins in a manner distinct from  
578 other studies. The researchers found that working even with the full virus was possible, and  
579 information on both the coat proteins, and the nucleic acids enclosed in the capsid could be  
580 obtained.<sup>100, 101</sup>

581 There are very few studies on the analysis of foodborne viruses by using Raman  
582 spectroscopy. Actually, there is a single study using Raman spectroscopy on Hepatitis A,  
583 which is the most common foodborne virus.<sup>105</sup> Hepatitis A 3C proteinase is known to be a

584 cysteine protease which is very important for the life cycle of this virus and responsible for  
585 the formation of mature viral proteins from the polyprotein precursor.<sup>106</sup> In the  
586 aforementioned research, Raman spectra were used to investigate acyl groups in the active  
587 site of the enzyme.<sup>105</sup> There have been several studies utilizing Raman spectroscopy for the  
588 investigation of Hepatitis viruses, but none of them have been reported as a foodborne  
589 virus.<sup>107-109</sup>

590

### 591 **Raman spectroscopy for toxin and chemical detection**

592 Contaminants are substances that have not been intentionally added to food. These substances  
593 may be present in foods as a result of contamination in any stage of the production,  
594 packaging, transport or storage. They can also result from the environmental contamination.  
595 Since contaminants in general have a negative impact on the quality of food and are a threat to  
596 human health<sup>110</sup>, a number of analytical methods have been developed for the identification  
597 and quantification of these compounds. Raman spectroscopy is one of these methods which  
598 has gained increasing attention in recent years. Specific Raman bands related to toxin and  
599 chemical detection were given in Table 6S.

600

### 601 **Toxins**

602 Brandt et al. aimed to study the structural properties of the toxins ricin, ricin agglutinin and  
603 ricin binding subunit B. Ricin and ricin agglutinin were extracted from *Ricinus communis*  
604 seeds and purified using affinity chromatography and gel-filtration. Vibrational bands of this  
605 plant toxin were then obtained by using Raman spectroscopy. Amide I at  $1640\text{ cm}^{-1}$ , amide III  
606 at  $1210\text{--}1300\text{ cm}^{-1}$ , a tyrosine doublet at  $830$  and  $855\text{ cm}^{-1}$ , bands for disulphide bridges at  
607  $510$ ,  $525$  and  $540\text{ cm}^{-1}$ , and some several bands corresponding to tryptophan amino acid

608 residues at  $1361\text{ cm}^{-1}$  were used as conformation sensitive bands for the molecules of  
609 interest.<sup>111</sup>

610 In another study, several vegetables and fruits were analysed with micro-Raman and  
611 near-infrared FT-Raman spectrometry to detect trace amounts of residual pesticides on the  
612 surface.<sup>112</sup> Bonora et. al., investigated the Raman spectra of atrazine, prometryn and simetryn  
613 herbicides in solid form and in polar and apolar solvents. A comparison was made between  
614 theoretical spectra and experimental spectra obtained from Raman and Surface-enhanced  
615 Raman spectroscopy (SERS) measurements.<sup>113</sup> In a similar study, Fleming et. al. investigated  
616 the molecular structure of phosphorus-containing herbicides. IR, Raman and SERS spectra  
617 were collected and compared with Density Functional Theory (DFT) calculations.<sup>114</sup>

618 Deoxynivalenol (DON) is one of the major secondary metabolites of the *Fusarium*  
619 genus and found predominantly in grains such as wheat, barley and corn.<sup>115</sup> The presence of  
620 DON degrades the quality of grain and has toxic effects on human health.<sup>116</sup> Traditional  
621 methods to measure DON concentrations in grain involve time-consuming steps such as  
622 extraction, washing and binding.<sup>117</sup> Due to the high moisture content in grain, broad intense  
623 water bands are yielded in both the IR and NIR regions. Thus, highly informative bands  
624 attributable to carbohydrate and protein species are inhibited. For this reason, various kinds of  
625 studies have been conducted with IR spectroscopy. The only study in the literature for  
626 identification of DON toxin by using a Raman technique with infrared spectroscopy was  
627 published by Liu et al.. In this study, feasibility of FT-Raman spectroscopy for the  
628 characterization and classification of ground wheat and barley contaminated with varying  
629 amounts of DON was investigated. PCA was performed in the spectral region  $1800\text{--}800\text{ cm}^{-1}$   
630 for multiplicative scatter correction of the Raman spectra. Principal component scores were  
631 then examined to discriminate between low and high DON in wheat.<sup>118</sup>

632 Raman spectroscopy coupled with LDA was used for qualitative and quantitative  
633 analysis of aflatoxin produced by *Aspergillus* in maize. Differences in the Raman bands were  
634 observed depending on the aflatoxin concentration in the samples.<sup>119</sup> In another study carried  
635 out by Lee et al., three different vibrational spectrophotometric methods, namely Raman, FT-  
636 NIR, and FT-IR were used for the detection of aflatoxin in different concentrations. By  
637 applying different chemometric methods to the spectra obtained from these three methods, a  
638 classification was made according to their aflatoxin quantities. The researchers stated that  
639 based on the results of the chemometric method they applied, Raman and FT-IR analyses had  
640 given relatively more satisfactory results compared to FT-NIR.<sup>120</sup>

641 In a study by Gupta et al., in situ synthesis of a nanopatterned conjugated molecularly  
642 imprinted polymer for bioagent T-2 on a bare gold chip and its integration with surface  
643 plasmon resonance and Raman spectroscopy were explored. The p-aminophenylboronic acid  
644 (p-APBA) and p-APBA with T-2 were characterized with Raman spectroscopy. Upon  
645 polymerization of p-APBA with T-2, the presence of new bands was detected, and they were  
646 assigned to symmetric B-O and asymmetric C-O stretching modes for p-APBA and T-2 in the  
647 sample.<sup>121</sup>

648

## 649 **Chemicals**

650 Coumarin is a naturally occurring benzopyrone found in most plants including tonka beans,  
651 sweet clover, woodruff and grass. It was used as a flavouring food additive until its direct use  
652 was banned due to the concerns about hepatotoxic effects on animal models.<sup>122</sup> Sortur et al.  
653 reported that IR and Raman spectra of 6-methyl-4-bromomethylcoumarin were obtained by  
654 following the reaction of *p*-cresol with 4-bromoethyl acetoacetate on an ice bath.<sup>123</sup>

655 Bisphenol A (BPA) is an estrogenic compound widely used in polycarbonate plastics,  
656 food cans and food storage containers.<sup>124</sup> Dybal and co-workers prepared BPA samples by

657 varying thermal and solvent treatments. Characteristic amorphous bands at 735 and 1235  $\text{cm}^{-1}$   
658 were used to determine the degrees of crystallinity of the BPA polycarbonate samples.<sup>125</sup>

659 Ground waters may be contaminated with perchlorate ions originating from the use of  
660 fertilizers and manufacturing activities. Levitskaia, Sinkov and Bryan used perchlorate loaded  
661 ion exchange resin as their model system. Determination of perchlorate with Raman  
662 spectroscopy was found to be a practical real time detection method. Perchlorate, a tetrahedral  
663 anion possessing easily polarizable Cl-O bonds, exhibits a vibrational frequency of the  
664 symmetric stretch near 934  $\text{cm}^{-1}$  in aqueous solution. The  $\text{ClO}_4^-$  bands were normalized to the  
665 intensity of the prominent A850 resin band at 1452  $\text{cm}^{-1}$  that served as an internal standard.<sup>126</sup>  
666 Yu et. al used RR spectroscopy for quantitative analysis of divalent metal ions.<sup>127</sup> Chelation  
667 property of zincon molecule with  $\text{Cu}^{2+}$  and  $\text{Ni}^{2+}$  enabled researchers to obtain complexes  
668 which could be followed by RR spectroscopy.

669 Polycyclic aromatic hydrocarbons (PAH) constitute a potential health danger because of  
670 their ability to induce carcinogenesis. PAH (such as naphthalene, anthracene, phenanthrene,  
671 and pyrene) could be detected in trace levels by making use of UV-RR spectrometry. A strong  
672 band for naphthalene was located at 766  $\text{cm}^{-1}$ . Other strong bands were observed at 399, 756  
673 and 1407  $\text{cm}^{-1}$  for anthracene, at 386, 745 and 1386  $\text{cm}^{-1}$  for phenanthrene and at 582, 1393,  
674 and 1622  $\text{cm}^{-1}$  for pyrene.<sup>128</sup> Alajtal, Edwards and Scowen used FT-Raman spectroscopy to  
675 investigate the effect of spectral resolution on the Raman spectra of several polyaromatic  
676 hydrocarbons. In this study, Raman measurements of beta-carotene naphthalene,  $\beta$ -carotene  
677 anthracene,  $\beta$ -carotene pyrene, and naphthalene, anthracene, and pyrene molecules were taken  
678 with different spectral resolutions. The effect of spectral resolution on the obtained Raman  
679 spectra was evaluated in this study.<sup>129</sup>

680 In the study of Sundaraganesan, Puviarasan and Mohan, the vibrational spectra of  
681 acrylamide found in starchy food products as a result of cooking practices was discussed in

682 detail with respect to various environments. A complete vibrational assignment using  
683 polarization data along with the results of normal coordinate analysis were presented in this  
684 study by taking into account the internal modes of the CH<sub>2</sub> and NH<sub>2</sub> groups.<sup>130</sup>

685

### 686 **Raman spectroscopy in food additive analysis**

687 Raman spectroscopy has also been used to detect food additives, and different approaches  
688 have been taken into account for this purpose. Specific Raman bands for food additive  
689 analysis section were given in Table 7S.

690 Astaxanthin (E-161j) and cantaxanthin (E-161g), the two major carotenoids responsible  
691 for the red-orange colour of salmon, were investigated by using Raman spectroscopy. Strong  
692 Raman signals were observed as a result of the C=C stretch vibrations of the carotenoid  
693 molecules.<sup>131</sup> Carbon black (E-153), another colouring agent which is produced by the  
694 combustion of hydrocarbons, was analysed with Raman spectroscopy.<sup>132</sup> Snehalatha et. al.,  
695 investigated the molecular structure of amaranth (E-123), a commonly used colouring agent  
696 of the food industry. Most characteristic bands were assigned to the vibrations of naphthalene  
697 ring and azo chromophoric group (C-N=N-C). A medium intensity band in the Raman  
698 spectrum was identified as the symmetric stretching vibration of the SO<sub>3</sub> group. The strongest  
699 Raman band was obtained out of the naphthalene ring vibrations.<sup>133</sup> Peica et. al. studied the  
700 molecular structure of tartrazine (E-102), an artificial dye which is also known for its potential  
701 to cause allergic reactions. Its strongest bands resulted from the azo and carboxyl groups and  
702 C-H deformation of the phenyl groups.<sup>134</sup> Curcumin is a natural coloring agent and  
703 stabilizer in the food industry as it is the major contributor to human health, yet it has a  
704 limited application area because of its low solubility and stability. To enhance solubility and  
705 stability of curcumin, encapsulation was applied with cyclodextrin, and then characterization  
706 of this complex was accomplished with Raman spectroscopy. The researchers showed that

707 Raman spectra of curcumin-cyclodextrin complex were different from Raman spectrum of  
708 curcumin.<sup>135</sup>

709 Zborowski et. al., used IR and Raman spectroscopy for characterizing the molecular  
710 structure of maltol which is widely used as a natural food additive. Maltol was characterized  
711 with its strong band related to the O-H stretching.<sup>136</sup> Peica et. al. used Raman spectroscopy to  
712 investigate the molecular structure of monosodium glutamate which is a commonly used  
713 flavour enhancer in various food products. Strong Raman bands were explained by CH<sub>2</sub>  
714 stretching, COO<sup>-</sup> stretching, CH<sub>2</sub> deformation, completely ionized form, and COO<sup>-</sup>  
715 twisting.<sup>137</sup> In another study by Peica et. al., aspartame (E-951) as an artificial sweetener was  
716 analysed by using Raman spectroscopy. Strong Raman bands were assigned to symmetrical  
717 C-H phenyl ring stretching, in-plane C-H phenyl ring bending, symmetrical stretching,  
718 phenylalanine ring stretching, CH<sub>3</sub> rocking, and skeletal deformation.<sup>138</sup>

719 Potential of IR, Raman and SERS to determine the excess azodicarbonamide additive in  
720 flour samples was evaluated. Its reaction products, namely biurea and semicarbazide that were  
721 formed during baking process were monitored by following their characteristic Raman  
722 spectra. Although multiple characteristic Raman bands were observed for each product, their  
723 presence is mostly assigned to the deformation bands of NH<sub>2</sub>, stretching and bending  
724 vibrations of N-C and C=O bounds. Results taken from experimental and calculated Raman  
725 spectra were verified with DFT.

726 Another food additive, chitosan, which is obtained by deacelitation of chitin, is of  
727 great importance since the degree of its deacetylation is vital in order to determine its chemical  
728 and physiccal properties such as solubility, biodergradibility and biocompatibility.<sup>139</sup> In this  
729 respect, Zajac et al. demonstated that the deacetylation degree of chitosan could be calculated  
730 by following certain bands obtained from Raman and IR spectra related to it.<sup>140</sup> The other  
731 chitosan derivative obtained by sulfating are known to have anticoagulant, antiviral,

732 antimicrobial, and antioxidant characteristics. It could be possible to determine the degree of  
733 substitution and to characterize sulfated chitosan compounds using Raman spectroscopy.  
734 Changes due to binding of sulfate groups to chitosan were detected in the obtained Raman  
735 spectra (1070, 1014, 823-834, 580-610, 2964  $\text{cm}^{-1}$ ) and these compounds were characterized  
736 according to the amount of the sulfate group attached to the structure.<sup>141</sup>

737 Another food additive is mannitol, which is used in the production of low-calorie food,  
738 as well as in the pharmaceutical industry and in other lyophilized products. In a study,  
739 changes occurring in the bands of ice, water and mannitol during the lyophilization of  
740 mannitol, were examined. Raman bands of ice and mannitol were monitored at the spectral  
741 regions 150-250  $\text{cm}^{-1}$  and 1000-1170  $\text{cm}^{-1}$ , respectively. Different polymorphic forms of  
742 mannitol were displayed during the lyophilization process.<sup>142</sup>

743

#### 744 **Raman spectroscopy in raw material analysis**

745 Rapid and *in situ* analysis of raw materials is one of the most important quality control  
746 applications in food industry. Assessing the quality of raw materials before the food production  
747 phase helps manufacturers save time and reduce the cost. Identification of raw materials is  
748 also essential due to its major effect on the quality of final product. Taking these requirements  
749 into account, it can be stated that Raman spectroscopy provides a wide range of applicaion  
750 area in which the raw material analysis constitutes a significant part. In this context, Raman  
751 spectroscopy has been widely used for raw material analysis, particularly for the  
752 discrimination of food samples, monitoring chemical and biochemical processes,  
753 compositional characterization of food samles and authentication of foods. Nevertheless,  
754 analyzing the Raman spectra of food samples mostly requires chemometric tools because of  
755 the complex structure of food matrix. Unsupervised chemometric methods like Principal

756 Component Analysis (PCA) and supervised chemometric methods like Partial Least Square  
757 (PLS), Partial Least Square-Discriminant Analysis (PLS-DA), Principal Component  
758 Regression (PCR) as well as Artificial Neural Networks (ANN) were generally employed for  
759 the detailed analysis of collected Raman data.<sup>143-146</sup> Specific Raman bands reported in the  
760 context of the reviewed articles is given in Table 8S for raw material analysis.

761

## 762 **Honey**

763 In a study by Goodacre, Radovic and Anklam, Raman spectroscopy was used with PCA and  
764 ANN to discriminate between honey samples provided from various European countries with  
765 different floral and geographical origins.<sup>144</sup> First, scores representing the Raman spectra of  
766 honey samples were obtained and then ANN, which was created from these scores, was used  
767 for discrimination. According to the results, 13 of 14 honey samples were classified  
768 accurately, but the country of origin was not predicted successfully as the number of honey  
769 samples was insufficient. Another research on honey has also recently been carried out by  
770 Özbalci et al. In this study, sugar contents of honey samples were quantified by applying  
771 chemometric methods to Raman spectra of honey samples.<sup>147</sup> Similar to the first study  
772 mentioned in this review, Carvucci et al. discriminated the honey samples collected from  
773 different regions by using Raman spectroscopy. They processed the Raman spectra that they  
774 obtained according to the pollen composition of genuine honey by using PCA, and identified  
775 the botanical and geographical origins of it.<sup>148</sup>

776

## 777 **Coffee**

778 There are three studies in the literature conducted for discriminating between Arabica and  
779 Robusta green coffee by using Raman spectroscopy.<sup>143, 149, 150</sup> The reason for the researchers  
780 to discriminate these two kinds coffee is that their quality, and thus price is not the same.

781 Analyzing their lipid content was the focus of these studies, and it was found that especially  
782 their kahweol content considerably differs from each other. The first Raman study on this  
783 topic of interest was carried out by using FT-Raman spectroscopy. The researchers obtained  
784 Raman spectra of lipid samples (kahweol and cafesto) extracted from coffee samples. Two  
785 characteristic peaks ( $1567$  ve  $1478\text{ cm}^{-1}$ ) of kahweole were found in the extract taken from  
786 Arabica coffee, which is specific to this type of coffee. They also discriminated between these  
787 two coffee types with a success rate of 93% by using chemometric method PCA.<sup>150</sup> Similarly,  
788 in a subsequent study, these two kinds of coffee were discriminated by using FT-Raman.  
789 However, it differs from the former study in that Raman spectra of the samples were taken  
790 without applying any chemical and physical procedure on the coffee beans. The discrimination  
791 of the coffees was performed by calculating the “spectral kahweol index” with the spectra  
792 obtained from the samples with different geographical origins.<sup>149</sup> In another study,  
793 chlorogenic acid rate was also examined as well as the lipids present in Arabica and Robusta  
794 green coffee. Raman spectra of the samples were obtained with visible micro-Raman  
795 spectroscopy; and by using two different PCA models, the discrimination of the coffees were  
796 accomplished with a success rate of 93%.<sup>143</sup>

797

### 798 **Lipid**

799 A study on discrimination among different edible oils and fats was performed by Yang et al.  
800 In this study, spectra obtained from FT-Raman spectroscopy were compressed with PLS and  
801 PCA; then the processed data were used for Linear Discriminant Analysis (LDA) and  
802 Canonical Variate Analysis (CVA). As a result of the analyses performed using the spectral  
803 range between  $400$  and  $3700\text{ cm}^{-1}$  (Table 1S), PLS-CVA was found to be the best method for  
804 discriminating edible oil and fats by FT-Raman, with calibration and validation data of 93.3%  
805 and 94.4%, respectively.<sup>68</sup> Korifi et al. tried to evaluate the capability of confocal Raman

806 spectroscopy combined with chemometric treatments to authenticate virgin olive oils with the  
807 protected designation of origin (PDO) label. Hence, PLS-DA was applied to the spectra of  
808 eight French PDOs, and 92.3% of these oils were accurately classified.<sup>151</sup> Raman  
809 spectroscopy has also been used to determine the quality of the olive fruit, which is one of the  
810 most important quality parameters in olive oil processing. In another study on olive oil, it was  
811 put forward that low-resolution portable Raman system could be utilized for determining  
812 oxidation states of oils. Having benefited from a chemometric method (PLS), the researchers  
813 stated that due to oxidation, changes occurred in the bands at about 1267, 1302, 1442, 1655 ve  
814 1747  $\text{cm}^{-1}$ .<sup>71</sup> They also tried to determine the quality of olive oil by using the Raman spectra  
815 of ground or sound olive paste, and then attempted to discriminate the origin of the olives as  
816 ground or sound. In the first stage of the study, PCA was used to find natural clusters in the  
817 Raman spectra, and then supervised classification methods, namely Soft Independent  
818 Modelling of Class Analogy (SIMCA), PLS-DA and *K*-Nearest Neighbors' (KNN) were  
819 applied. The best results for classification were found in the KNN method, with prediction  
820 abilities of 100% for sound and 97% for ground olives in an independent validation set. In this  
821 study, it was demonstrated that portable Raman spectroscopy can be utilized to determine the  
822 quality of olives used in the production of olive oils in the field.<sup>152</sup> Different from the other  
823 studies on olive oil, Gouvinhas et al., produced extra virgin olive oil by means of taking  
824 samples from three types of olive in different stages of their ripening periods. They were  
825 classified according to their types and ripening periods through processing the Raman spectra  
826 with qualitative methods. It was found that 1749, 1651, 1439, 1303 ve 1267  $\text{cm}^{-1}$  bands  
827 obtained from Raman measurements directly demonstrates the fatty acid contents of the  
828 samples, and changes were observed in the intensities due to ripening.<sup>153</sup>  
829

830 In another study, different types of pure animal fat (poultry, pig, bovine, and lamb and  
831 fish oils) and mixture samples of them were classified according to their origin by using PCA  
832 and PLS-DA analyses.<sup>66</sup> The same analysis was performed with different types of edible fats.  
833 Fish, poultry, pig and bovine fats were well distinguished by applying PCA. Using PLS-DA  
834 analysis, poultry, pig and bovine fat samples were discriminated with high sensitivity and  
835 specificity values and with few classification errors. In addition, types of edible fats like fish  
836 oils and acidic oils from chemical or physical refining could also be discriminated with PLS-  
837 DA.<sup>66</sup> Velioglu et al., used Raman spectroscopy to assess the freshness of fish samples  
838 according to the number of freezing/thawing cycles they were exposed to. PCA was employed  
839 to cluster the samples according to their freshness. Changes in the intensities of the  
840 characteristic Raman bands were mostly attributed to the alterations in the lipid structure.<sup>154</sup>  
841 Potential of Raman spectroscopy to predict the purity of caviars was evaluated. Linear  
842 methods such as PCA and LDA as well as non-linear methods such as ANN were used to  
843 classify different caviar samples according to their purity and type. More accurate predictions  
844 were obtained by using the ANN with 91.4% of prediction capability. Fatty acids and fat  
845 contents of the caviar samples was quantified through Raman spectroscopy coupled with PLS  
846 regression.<sup>155</sup>

847 In addition to the abovementioned studies on lipids, there is another study in which  
848 Raman spectra of 35 lipids belonging to different families (saturated and unsaturated fatty  
849 acids, triacylglycerols, cholesterol, cholesteryl esters and phospholipids) were obtained. It was  
850 found that Raman spectra of each of these lipids display changes depending on their  
851 saturation state, their being in liquid and solid state, and on isomer forms. The characteristic  
852 features of Raman spectra is attributable to the existence of hydrocarbon chains, and they  
853 were observed at 1500-1400, 1300-1250, 1200-1050, 3000-2800  $\text{cm}^{-1}$ , respectively, which  
854 was caused by C–C and C–H stretching modes and the scissoring and twisting vibrations of

855 CH<sub>2</sub> and CH<sub>3</sub> groups. Besides, lipids belonging to each group was found to have characteristic  
856 bands specific to them.<sup>156</sup>

857

### 858 **Fermentation products**

859 Raman spectroscopy can also be used to detect materials such as ethanol, lactic acid, and  
860 acetic acid that are produced as a result of processes like fermentation. Sivakesava et al.,  
861 followed ethanol fermentation by *Saccharomyces cerevisiae* (*S. cerevisiae*) using Fourier  
862 Transform-Middle Infrared (FT-MIR) and FT-Raman spectroscopy. In this study, quantities  
863 of glucose, ethanol and the optical cell density of *S. cerevisiae* during fermentation were  
864 investigated using chemometric methods.<sup>157</sup> In another study, FT-MIR, Fourier Transform-  
865 Near Infrared (FT-NIR) and FT-Raman spectroscopy were used during lactic acid  
866 fermentation to determine quantities of the same parameters as the previous study of  
867 *Lactobacillus casei* (*L. casei*).<sup>158</sup> Similarly, quantitative measurements of glucose during  
868 ethanol fermentation in the beverage industry were carried out by Delfino et al.<sup>37</sup> Our research  
869 group has also monitored a two-step acetic acid fermentation in a study using Raman  
870 spectroscopy. The first step was consumption of sugars in a grape juice mixture and then  
871 formation of alcohol by *S. cerevisia*. The second step was carried out with *Acetobacter aceti*  
872 that converted the alcohol to acetic acid.<sup>159</sup> Wang et al. used Raman Spectroscopy to monitor  
873 the consumption and formation of glucose, glycerol and ethanol during wine fermentation.  
874 HPLC was used for the validation analysis.<sup>160</sup> Micro-Raman spectroscopy was used to follow  
875 the fermentation process during yoghurt production. Chemical transformation of lactose and  
876 inorganic phosphorus into lactic acid and organic phosphorus and the formation of the  
877 exopolysaccharides were monitored based on the collected Raman spectra as a function of the  
878 incubation time.<sup>161</sup>

879

**880 Other foods**

881 A dispersive Raman spectroscopic method was developed to determine protein and oil  
882 contents of soybeans.<sup>162</sup> Optimal prediction models were generated by PLS algorithms based  
883 on collected Raman spectra (200-1800  $\text{cm}^{-1}$ ) of the samples. Protein and oil content of the  
884 soybeans were successfully predicted with high  $R^2$  values (0.916 and 0.872 for protein and oil  
885 contents, respectively). Characterization of foods is another topic studied by using Raman  
886 spectroscopy. For this purpose, FT-Raman spectroscopy was used for the characterization of  
887 Marama beans from Southern Africa. Both quantitative and qualitative data on the  
888 composition of Marama bean oil, including carbohydrates, proteins, amino acids and aromatic  
889 compounds, were obtained.<sup>145</sup> Ripe and unripe tomato fruit samples were analyzed with  
890 portable and confocal Raman microscope to obtain spectral data on their main organic  
891 components. Two different laser excitation wavelengths were used for confocal microscope  
892 measurements to maximize the obtained spectral information.<sup>163</sup> By using spectral data, cutin  
893 and cutinal waxes on unripe tomatoes and carotenes, and polyphenoles and polysaccharides  
894 on ripe tomatoes were identified as major compounds. In another study, the researchers traced  
895 the lycopene formation and distribution in the structures of the harvested tomatoes during  
896 different stages (green, breaker, turning, pink, light red, red) of their ripening period by using  
897 Raman chemical imaging. Tomatoes in different ripening periods were cut parallel to the  
898 plane, and Raman spectra were taken from their seeds, locular tissues and outer pericarps. As  
899 a result of the trials, two basic peaks (1151 and 1513  $\text{cm}^{-1}$ ) belonging to lycopene were  
900 detected both in locular tissues and on outer pericarps of fully ripened (red) tomatoes.<sup>164</sup>  
901 Gonzalves et. al., used transmission resonance Raman spectroscopy to investigate the spatial  
902 distribution of carotenoids in carrot roots, and they found that the changes in the intensities of  
903 Raman bands obtained from different parts of carrots were attributed to molecular

904 configuration of  $\beta$ -carotene. As a consequence,  $\beta$ -carotene showed a heterogenous  
905 distribution, and seen particularly in the secondary phloem tissue, and periderm.<sup>165</sup>

906 Raman spectroscopy can also be used to monitor important components such as ethanol,  
907 lactic acid, and acetic acid produced during fermentation<sup>166,167</sup> and/or spoilage of foods<sup>168</sup> and  
908 chemical and biochemical transformations.<sup>169, 170</sup>

909

### 910 **Raman spectroscopy to detect food adulteration**

911 Food is adulterated by unscrupulous producers in order to benefit economically from  
912 falsifying food information. The development of new techniques to verify food safety and  
913 authenticity has been an important issue thanks to the increasing consumer awareness.<sup>1</sup> For  
914 this reason, rapid and eco-friendly techniques have replaced time-consuming and tiresome  
915 chemical and traditional reference methods. As a vibrational technique, Raman spectroscopy  
916 is one of the analytical tools and is attracting growing attention due to its ability to provide  
917 fingerprint characteristics of food products and its offering a rapid, non-destructive and cheap  
918 analysis. In addition, quantitative and qualitative information can be obtained from a  
919 combination of Raman spectroscopy with multivariate data analyses.<sup>171</sup> Specific Raman bands  
920 of related articles to this section were given in Table 9S for food adulteration.

921 Zou et al. used a portable Raman spectroscopy to distinguish between genuine olive oil  
922 and the oil adulterated with low quality oils. A method was developed based on the  
923 normalization of *cis*-(=C-H) and *cis*-(C=C) bands intensities at 1265  $\text{cm}^{-1}$  and 1657  $\text{cm}^{-1}$ , by  
924 the  $\text{CH}_2$  band intensity at 1441  $\text{cm}^{-1}$ . Adulterated olive oil containing as little as 5% (v/v) or  
925 more of other edible oils have been successfully detected in the relevant study.<sup>172</sup> Zhang et al.  
926 investigated extra virgin olive oils adulterated with soybean, corn or sunflower seed oil by  
927 characterizing their Raman spectra in the 1000–1800  $\text{cm}^{-1}$  range. The Raman spectra were  
928 normalized according to the  $\text{CH}_2$  band of the oil samples. An external standard method (ESM)

929 was applied to achieve quantitative analysis and compared with the results of SVM methods.  
930 Potential of ESM based on Raman spectroscopy to detect olive oil adulteration was shown in  
931 this study.<sup>173</sup> In another study of Zhang et al., the level of adulteration in a set of olive oil  
932 samples containing 5% or more of different types of oils such as soybean, rapeseed, sunflower  
933 and corn oil was successfully determined. Using PCA made it possible to obtain a clear  
934 separation of oil samples according to their different mono-unsaturated fatty acid,  
935 polyunsaturated fatty acid, and saturated fatty acid contents.<sup>174</sup> Lopez-Diez et al. also  
936 investigated the authentication of various extra virgin olive oils, and their adulteration with  
937 hazelnut oil by using Raman spectroscopy. The obtained Raman spectra were normalized  
938 according to the frequency of the band representing the scissoring-bending mode of  $-\text{CH}_2$   
939 groups. The spectra were examined by using PCA, PLS and Genetic Programming. Extra  
940 virgin olive oils from different parts of the Italian peninsula and their mixtures with hazelnut  
941 oils were characterized using PCA. The PLS method was also used as a predictive linear  
942 model.<sup>175</sup> El-Abassy et al. studied visible Raman spectroscopy to classify different vegetable  
943 oils and quantify the adulteration of virgin olive oil with sunflower oil. PCA was used for the  
944 classification study, while PLS regression analysis was used to monitor the adulteration.  
945 Quantitative detection limit was decreased to 500 ppm (0.05%), which is significant in the  
946 case of allergic reactions.<sup>176</sup> Adulteration of extra virgin olive oil with olive pomace oil was  
947 determined by means of NIR, FT-IR and FT-Raman spectroscopy. PLS was used to  
948 quantitatively analyse the olive oil samples adulterated with different rates of olive pomace  
949 oil.<sup>177</sup> Baeten and Aparicio conducted European project FAIR-CT96-5053, which evaluated  
950 the performance of FT-Raman, NIR and FT-MIR spectroscopy to authenticate one-hundred  
951 thirty-eight different edible oil and fat samples.<sup>178</sup> PCA and stepwise linear discriminant  
952 analysis (SLDA) methods were performed to classify oils and fats by conducting cluster and  
953 discriminant analyses. Three clusters of samples that were rich in saturated fatty acids,

954 monounsaturated fatty acids or polyunsaturated fatty acids were obtained with PCA according  
955 to the degree of unsaturation of the oils. In another method, SLDA was performed to classify  
956 edible oils and fats according to their sources, and to quantify virgin olive oil adulteration. In  
957 one of the studies reported by our research group, Raman spectroscopy was used to detect the  
958 adulteration in butter samples spiked with margarine. Prediction success of the models  
959 created by using different chemometric methods namely PCA, PCR, PLS and ANN were  
960 compared.<sup>179</sup>

961 Adulteration of milk powder with melamine was determined quantitatively by using  
962 portable Raman spectroscopy coupled with PLS regression. Melamine adulteration was  
963 monitored using the characteristic bands of melamine located at one strong band at  $673\text{ cm}^{-1}$   
964 and a weak band at  $982\text{ cm}^{-1}$ . The intensity of the band at  $673\text{ cm}^{-1}$  was used for quantification  
965 of melamine concentration in milk powder.<sup>180</sup> In a similar study, adulteration of milk powder  
966 with melamine was examined using the melamine band located at  $676\text{ cm}^{-1}$ .<sup>181</sup> Adulteration  
967 was successfully determined in the milk powder samples spiked with calcium carbonate.  
968 Prominent peak of calcium carbonate located at  $1085\text{ cm}^{-1}$  was followed in FT-Raman spectra  
969 of milk powder samples. PCA and PLS was used with Raman spectroscopic data to quantify  
970 the adulteration rate.<sup>182</sup> Multiple adulterants, namely ammonium sulphate, dicyandiamide,  
971 melamine, and urea present in the milk powder samples were simultaneously detected by  
972 using Raman chemical imaging coupled with mixture analysis algorithms. Differences in the  
973 Raman spectra of four chemical adulterants allowed researchers to detect and differentiate  
974 these compounds. The strongest Raman bands characterizing the relevant chemical  
975 compounds were as follows;  $973\text{ cm}^{-1}$  for ammonium sulphate,  $212\text{ cm}^{-1}$  for dicyandiamide,  
976  $673\text{ cm}^{-1}$  for melamine and  $1009\text{ cm}^{-1}$  for urea.<sup>183</sup>

977 Adulteration of maple syrup with corn syrup has been investigated using FT-IR, FT-  
978 Raman and NIR spectroscopy. Quantitative analyses of adulterated samples were performed

979 with PLS. PCA-LDA, PLS-CVA, PLS-LDA and PCA-CVA methods were also applied for  
980 discriminant analysis, but the best results were obtained with PCA-CVA. Characteristic bands  
981 mostly attributed to the presence of carbohydrates were used for creating above-mentioned  
982 predictive models.<sup>184</sup>

983 Adulterated honey samples with various floral origins containing beet and cane inverts  
984 were successfully determined using FT-Raman spectroscopy coupled with PLS and PCA  
985 combined with CVA and LDA.<sup>146</sup>

986 Detection of paraffin in the adulterated rice samples was investigated. Confocal  
987 microscope Raman measurements were performed on the surface of rice samples to obtain  
988 information about chemical composition. PCA, SIMCA, PLS-DA, KNN and SVM methods  
989 were used to differentiate rice samples from different locations and to detect paraffin in the  
990 adulterated rice samples. Although the Raman spectra of rice samples comprised of starch,  
991 protein and lipid, researchers were also able to detect the presence of paraffin by following  
992 the strong Raman bands at 1062, 1132, 1295, 1417, 1440 and 1462  $\text{cm}^{-1}$ .<sup>185</sup>

993 Methanol and ethanol content of distilled alcoholic beverages was successfully  
994 determined with Raman spectroscopy. Quantification of methanol in mixtures was done using  
995 the intensities of methanol and ethanol bands located at 1019 and 879  $\text{cm}^{-1}$ , respectively.  
996 Collected Raman data was normalized by using acetonitrile as an internal standard in the  
997 developed method.<sup>186</sup> Nguyen and Wu developed a Raman spectroscopic method to quantify  
998 low concentrations of methanol in alcohol. PLS regression was applied to the collected  
999 Raman spectra where spectral region between 950 and 1200  $\text{cm}^{-1}$  was specifically used to  
1000 obtain the calibration curves.<sup>187</sup>

1001 Identification of meat species is of great importance in order to determine the potential  
1002 adulteration of meat products with cheaper alternatives. Beattie et. al., used Raman  
1003 spectroscopy and multivariate data analysis to classify adipose tissue samples from different

1004 origins. PLS-DA and PC-LDA were employed to classify the samples of chicken, beef, lamb  
1005 and pork species.<sup>188</sup> Sowoidnich et. al. used shifted excitation Raman difference spectroscopy  
1006 for the non-invasive differentiation of meat species, namely beef, pork, chicken and turkey. A  
1007 clear separation was obtained by employing PCA to the collected Raman data.<sup>189</sup> Boyaci et.  
1008 al., used Raman spectroscopy in combination with chemometrics to determine the beef  
1009 adulteration with horsemeat. Employing PCA on collected Raman data enabled researchers to  
1010 differentiate beef samples spiked with different rates of horsemeat.<sup>190</sup> In a similar study  
1011 reported by the same research group, extracted fat samples were used to differentiate meat  
1012 species namely, cattle, sheep, pig, fish, poultry, goat and buffalo. Salami products with  
1013 different formulations prepared by using these meat species were also investigated with  
1014 Raman spectroscopy.<sup>191</sup> Zajac et. al. used IR and FT-Raman spectroscopy to analyze the  
1015 amino acid composition of the samples in order to determine the content of horse meat in its  
1016 mixture with beef.<sup>192</sup>

1017

## 1018 **Conclusion**

1019 The use of Raman spectroscopy in food analysis is still in its initial stage despite its great  
1020 potential in almost every field of food science. Raman has many advantages compared to  
1021 other food analysis methods, and the use of Raman is increasing day by day. Raman  
1022 spectroscopy can replace traditional food analyses as it does not require labelling and pre-  
1023 treatment steps. In addition, Raman spectroscopy is a sensitive, reliable, non-destructive and  
1024 real-time method. Some important issues that need to be addressed for making Raman  
1025 spectroscopy a more commonly used method are:

1026 *a. Investigating the applications for Raman spectroscopy in food analysis.* Due to some  
1027 reasons (cost and scarcity of the instrument in food area etc.), the usage of the Raman  
1028 system in food analysis didn't use to be a common practice. Over the last two decades,

1029 however, these limitations have been partially eliminated, and the number of reported  
1030 studies in this field has increased. Nevertheless, it is still not sufficient and more studies  
1031 should be conducted. Results of the Raman system should be correlated with standard  
1032 methods, and new standard methods should be developed using Raman spectroscopy.

1033 According to our detailed research on the literature, some aspects of food analysis still  
1034 need to be investigated by using Raman spectroscopy. To our knowledge, mineral and  
1035 toxin analysis in food studies are among these aspects waiting to be dealt with using  
1036 Raman spectroscopy.

1037 *b. Application-driven databases for common analysis.* Although some studies have been  
1038 carried out in this field, there is still no available database related to Raman  
1039 spectroscopy in food analysis. Complex food matrices and variations in the systems  
1040 cause difficulties in preparation of databases. In this review, Raman bands obtained in  
1041 food analyses were summarized in tables (Table 1S-9S). We believe that these tables  
1042 will be beneficial for researchers in this field. However, more systematic experimental  
1043 work is needed for the preparation of this database. The Raman system's becoming  
1044 more widespread in food field will help develop a database.

1045 *c. Improving analysis efficiency.* The complex nature of the food sample reduces  
1046 efficiency of the analysis. To overcome this difficulty, some easy preprocessing  
1047 practices could be conducted before Raman measurement. In addition, novel data  
1048 processing techniques (chemometric methods and artificial neural networks) will be of  
1049 more help to the user, and processing Raman spectra with these methods will increase  
1050 the efficiency of the analysis.

1051 *d. Better analyser instrument.* Most of the Raman systems were developed for the  
1052 research purposes in laboratories. There is no individual Raman system for specific food  
1053 analysis. The success of Raman spectroscopy in food analysis will be increased through

1054 developing individual Raman systems. Field assays are also very important in food  
1055 analysis. Portable Raman systems have big potential in this field. Developments in light  
1056 source and detector technologies will help produce small size portable Raman modules  
1057 with better performance.

1058 *e. Low cost analyser system.* High cost of Raman modules obstructs the common usage  
1059 of the system in this field. Simpler systems, designed specifically for the sample and  
1060 portable Raman system should be produced with lower instrumentation cost.

1061 Raman spectroscopy in food analysis is receiving a lot of interest from researchers  
1062 worldwide. We believe that Raman spectroscopy will be one of the most common  
1063 methods to be used in food analysis in the near future.

1064

## 1065 SUPPLEMENTARY DATA AVAILABLE

1066 Supplementary data including the tables displaying the Raman bands of food components  
1067 (proteins, carbohydrates, lipids, and vitamins), microorganisms and viruses, toxins and  
1068 chemicals, food additives, raw materials and food adulterant is available.

1069

## 1070 Notes and References

- 1071 1. L. M. Reid, C. P. O'Donnell and G. Downey, *Trends Food Sci Tech*, 2006, **17**, 344-353.
- 1072 2. C. N. G. Scotter, *Trends Food Sci Tech*, 1997, **8**, 285-292.
- 1073 3. D. T. Yang and Y. B. Ying, *Appl Spectrosc Rev*, 2011, **46**, 539-560.
- 1074 4. A. Rohman and Y. B. C. Man, *Food Rev Int*, 2012, **28**, 97-112.
- 1075 5. R. J. Dijkstra, F. Ariese, C. Gooijer and U. A. T. Brinkman, *Trac-Trend Anal Chem*, 2005, **24**,  
1076 304-323.
- 1077 6. R. L. McCreery, in *Raman Spectroscopy for Chemical Analysis*, Wiley-Interscience, New York,  
1078 2000, pp. 251-291.
- 1079 7. B. J. Marquardt and J. P. Wold, *Lebensm-Wiss Technol*, 2004, **37**, 1-8.
- 1080 8. H. W. Wong, S. M. Choi, D. L. Phillips and C. Y. Ma, *Food Chem*, 2009, **113**, 363-370.
- 1081 9. A. M. Herrero, *Food Chem*, 2008, **107**, 1642-1651.
- 1082 10. D. Yang and Y. Ying, *Appl Spectrosc Rev*, 2012, **46**, 539-560.
- 1083 11. E. F. Olsen, C. Baustad, B. Egelandsdal, E. O. Rukke and T. Isaksson, *Meat Sci*, 2010, **85**, 1-6.
- 1084 12. A. M. Herrero, *Crit Rev Food Sci*, 2008, **48**, 512-523.
- 1085 13. H. Schulz and M. Baranska, *Vib Spectrosc*, 2007, **43**, 13-25.
- 1086 14. R. Tuma, *J Raman Spectrosc*, 2005, **36**, 307-319.

- 1087 15. E. G. Ferrer, A. V. Gomez, M. C. Anon and M. C. Puppo, *Spectrochim Acta A*, 2011, **79**, 278-  
1088 281.
- 1089 16. L. Liao, Q. Wang and M. M. Zhao, *J Sci Food Agr*, 2012, **92**, 1865-1873.
- 1090 17. S. Ngarize, A. Adams and N. K. Howell, *Food Hydrocolloid*, 2004, **18**, 49-59.
- 1091 18. T. W. Barrett, W. L. Peticolas and R. M. Robson, *Biophys J*, 1978, **23**, 349-358.
- 1092 19. Z. H. Chi, X. G. Chen, J. S. W. Holtz and S. A. Asher, *Biochemistry-Us*, 1998, **37**, 2854-2864.
- 1093 20. C. Y. Huang, G. Balakrishnan and T. G. Spiro, *J Raman Spectrosc*, 2006, **37**, 277-282.
- 1094 21. M. Nonaka, E. Lichan and S. Nakai, *J Agr Food Chem*, 1993, **41**, 1176-1181.
- 1095 22. N. Howell and E. LiChan, *Int J Food Sci Tech*, 1996, **31**, 439-451.
- 1096 23. I. Sanchez-Gonzalez, P. Carmona, P. Moreno, J. Borderias, I. Sanchez-Alonso, A. Rodriguez-  
1097 Casado and M. Careche, *Food Chem*, 2008, **106**, 56-64.
- 1098 24. X.-L. Xu, M.-Y. Han, Y. Fei and G.-H. Zhou, *Meat Sci.*, 2011, **87**, 159-164.
- 1099 25. D. T. Berhe, A. J. Lawaetz, S. B. Engelsen, M. S. Hviid and R. Lametsch, *Food Control*, 2015, **52**,  
1100 119-125.
- 1101 26. Z. L. Lim, N. H. Low, B. A. Moffatt and G. R. Gray, *Cryobiology*, 2013, **66**, 156-166.
- 1102 27. S. Pieters, Y. Vander Heyden, J.-M. Roger, M. D'Hondt, L. Hansen, B. Palagos, B. De  
1103 Spiegeleer, J.-P. Remon, C. Vervaet and T. De Beer, *Eur. J. Pharm. Biopharm.*, 2013, **85**, 263-  
1104 271.
- 1105 28. H.-W. Wong, S.-M. Choi, D. L. Phillips and C.-Y. Ma, *Food Chemistry*, 2009, **113**, 363-370.
- 1106 29. Z. L. Kang, P. Wang, X. L. Xu, C. Z. Zhu, K. Li and G. H. Zhou, *Meat Sci.*, 2014, **98**, 171-177.
- 1107 30. J.-H. Shao, Y.-F. Zou, X.-L. Xu, J.-Q. Wu and G.-H. Zhou, *Food Res. Int.*, 2011, **44**, 2955-2961.
- 1108 31. G. T. Meng, J. C. K. Chan, D. Rousseau and E. C. Y. Li-Chan, *J Agr Food Chem*, 2005, **53**, 845-  
1109 852.
- 1110 32. A. S. Sivam, D. Sun-Waterhouse, C. O. Perera and G. I. N. Waterhouse, *Food Res. Int.*, 2013,  
1111 **50**, 574-585.
- 1112 33. A. V. Gómez, E. G. Ferrer, M. C. Añón and M. C. Puppo, *J. Mol. Struct.*, 2013, **1033**, 51-58.
- 1113 34. N. Perisic, N. K. Afseth, R. Ofstad, S. Hassani and A. Kohler, *Food Chem*, 2013, **138**, 679-686.
- 1114 35. D. W. Gruenwedel and J. R. Whitaker, *Food analysis : principles and techniques*, Dekker, New  
1115 York, 1984.
- 1116 36. M. R. Almeida, R. S. Alves, L. B. L. R. Nascimbem, R. Stephani, R. J. Poppi and L. F. C. de  
1117 Oliveira, *Anal Bioanal Chem*, 2010, **397**, 2693-2701.
- 1118 37. I. Delfino, C. Camerlingo, M. Portaccio, B. Della Ventura, L. Mita, D. G. Mita and M. Lepore,  
1119 *Food Chem*, 2011, **127**, 735-742.
- 1120 38. K. Ilaslan, I. H. Boyaci and A. Topcu, *Food Control*, 2015, **48**, 56-61.
- 1121 39. M. Roman, J. C. Dobrowolski, M. Baranska and R. Baranski, *J Nat Prod*, 2011, **74**, 1757-1763.
- 1122 40. A.-S. Jääskeläinen, U. Holopainen-Mantila, T. Tamminen and T. Vuorinen, *J. Cereal Sci.*, 2013,  
1123 **57**, 543-550.
- 1124 41. L. Scudiero and C. F. Morris, *J. Cereal Sci.*, 2010, **52**, 136-142.
- 1125 42. N. Wellner, D. M. R. Georget, M. L. Parker and V. J. Morris, *Starch-Starke*, 2011, **63**, 128-138.
- 1126 43. N. Linlaud, E. Ferrer, M. a. C. Puppo and C. Ferrero, *J Agr Food Chem*, 2010, **59**, 713-719.
- 1127 44. M. S. Mikkelsen, B. M. Jespersen, F. H. Larsen, A. Blennow and S. B. Engelsen, *Food Chem*,  
1128 **2013**, **136**, 130-138.
- 1129 45. C. K. Chong, J. Xing, D. L. Phillips and H. Corke, *J Agr Food Chem*, 2001, **49**, 2702-2708.
- 1130 46. D. L. Wetzal, Y. C. Shi and U. Schmidt, *Vib Spectrosc*, 2010, **53**, 173-177.
- 1131 47. N. Dupuy and J. Laureyns, *Carbohydr Polym*, 2002, **49**, 83-90.
- 1132 48. L. Passauer, H. Bender and S. Fischer, *Carbohydr Polym*, 2010, **82**, 809-814.
- 1133 49. B. Volkert, A. Lehmann, T. Greco and M. H. Nejad, *Carbohydr Polym*, 2010, **79**, 571-577.
- 1134 50. E. Pigorsch, *Starch-Starke*, 2009, **61**, 129-138.
- 1135 51. S. N. Yuen, S. M. Choi, D. L. Phillips and C. Y. Ma, *Food Chem*, 2009, **114**, 1091-1098.
- 1136 52. K. C. Schuster, E. Urlaub and J. R. Gapes, *J Microbiol Meth*, 2000, **42**, 29-38.
- 1137 53. P. M. Fechner, S. Wartewig, P. Kleinebudde and R. H. H. Neubert, *Carbohydr Res*, 2005, **340**,  
1138 2563-2568.

- 1139 54. A. Flores-Morales, M. Jimenez-Estrada and R. Mora-Escobedo, *Carbohydr Polym*, 2012, **87**, 61-  
1140 68.
- 1141 55. C. Mutungi, L. Passauer, C. Onyango, D. Jaros and H. Rohm, *Carbohydr Polym*, 2012, **87**, 598-  
1142 606.
- 1143 56. M. I. U. Islam and T. A. G. Langrish, *Food Res. Int.*, 2010, **43**, 46-56.
- 1144 57. H. Akinosho, S. Hawkins and L. Wicker, *Carbohydr Polym*, 2013, **98**, 276-281.
- 1145 58. R. Kizil and J. Irudayaraj, *J Sci Food Agr*, 2007, **87**, 1244-1251.
- 1146 59. M. Łabanowska, A. Weselucha-Birczyńska, M. Kurdziel and P. Puch, *Carbohydr Polym*, 2013,  
1147 **92**, 842-848.
- 1148 60. J. Huen, C. Weikusat, M. Bayer-Giraldi, I. Weikusat, L. Ringer and K. Losche, *J Cereal Sci*, 2014,  
1149 **60**, 555-560.
- 1150 61. H. Sadeghijrabchi, P. J. Hendra, R. H. Wilson and P. S. Belton, *J Am Oil Chem Soc*, 1990, **67**,  
1151 483-486.
- 1152 62. F. L. Silveira, L. Silveira, A. B. Villaverde, M. T. T. Pacheco and C. A. Pasqualucci, *Instrum Sci*  
1153 *Technol*, 2010, **38**, 107-123.
- 1154 63. R. M. El-Abassy, P. J. Eravuchira, P. Donfack, B. von der Kammer and A. Materny, *Vib.*  
1155 *Spectrosc.*, 2011, **56**, 3-8.
- 1156 64. C. M. McGoverin, A. S. S. Clark, S. E. Holroyd and K. C. Gordon, *Anal Chim Acta*, 2010, **673**, 26-  
1157 32.
- 1158 65. J. R. Beattie, S. E. J. Bell, C. Borggaard, A. M. Fearon and B. W. Moss, *Lipids*, 2004, **39**, 897-906.
- 1159 66. O. Abbas, J. A. F. Pierna, R. Codony, C. von Holst and V. Baeten, *J. Mol. Struct.*, 2009, **924-26**,  
1160 294-300.
- 1161 67. V. Baeten, P. Hourant, M. T. Morales and R. Aparicio, *J Agr Food Chem*, 1998, **46**, 2638-2646.
- 1162 68. H. Yang, J. Irudayaraj and M. M. Paradkar, *Food Chem*, 2005, **93**, 25-32.
- 1163 69. B. Muik, B. Lendl, A. Molina-Díaz and M. J. Ayora-Canada, *Chem Phys Lipids*, 2005, **134**, 173-  
1164 182.
- 1165 70. P. Kathirvel, I. V. Ermakov, W. Gellermann, J. Mai and M. P. Richards, *Int J Food Sci Tech*,  
1166 2008, **43**, 2095-2099.
- 1167 71. E. Guzmán, V. Baeten, J. A. F. Pierna and J. A. Garcia-Mesa, *Food Control*, 2011, **22**, 2036-  
1168 2040.
- 1169 72. I. Sanchez-Alonso, P. Carmona and M. Careche, *Food Chem*, 2012, **132**, 160-167.
- 1170 73. Y. Fan, J. Zhou and D. P. Xu, *Spectrochim Acta A*, 2014, **129**, 143-147.
- 1171 74. R. Rodríguez-Solana, D. J. Daferera, C. Mitsi, P. Trigas, M. Polissiou and P. A. Tarantilis, *Ind.*  
1172 *Crops Prod.*, 2014, **62**, 22-33.
- 1173 75. R. M. El-Abassy, P. Donfack and A. Materny, *Food Res Int*, 2010, **43**, 694-700.
- 1174 76. S. Ötleş, *Methods of analysis of food components and additives*, CRC Press, Boca Raton, 2005.
- 1175 77. L. Rimai, D. Gill and J. L. Parsons, *J Am Chem Soc*, 1971, **93**, 1353-&.
- 1176 78. C. Y. Panicker, H. T. Varghese and D. Philip, *Spectrochim Acta A*, 2006, **65**, 802-804.
- 1177 79. C. W. Tsai and M. D. Morris, *Anal Chim Acta*, 1975, **76**, 193-198.
- 1178 80. C. Cimpoiu, D. Casoni, A. Hosu, V. Miclaus, T. Hodisan and G. Damian, *J Liq Chromatogr R T*,  
1179 2005, **28**, 2551-2559.
- 1180 81. M. Kim and P. R. Carey, *J Am Chem Soc*, 1993, **115**, 7015-7016.
- 1181 82. J. R. Beattie, C. Maguire, S. Gilchrist, L. J. Barrett, C. E. Cross, F. Possmayer, M. Ennis, J. S.  
1182 Elborn, W. J. Curry, J. J. McGarvey and B. C. Schock, *Faseb J*, 2007, **21**, 766-776.
- 1183 83. H. Yang and J. Irudayaraj, *J Pharm Pharmacol*, 2002, **54**, 1247-1255.
- 1184 84. V. Velusamy, K. Arshak, O. Korostynska, K. Oliwa and C. Adley, *Biotechnol Adv*, 2010, **28**, 232-  
1185 254.
- 1186 85. M. Koopmans, C. H. von Bonsdorff, J. Vinje, D. de Medici and S. Monroe, *Fems Microbiol Rev*,  
1187 2002, **26**, 187-205.
- 1188 86. P. Rösch, M. Schmitt, W. Kiefer and J. Popp, *J. Mol. Struct.*, 2003, **661**, 363-369.
- 1189 87. H. Yang and J. Irudayaraj, *J. Mol. Struct.*, 2003, **646**, 35-43.

- 1190 88. S. Stockel, S. Meisel, R. Bohme, M. Elschner, P. Rosch and J. Popp, *J Raman Spectrosc*, 2009,  
1191 **40**, 1469-1477.
- 1192 89. K. Maquelin, L. P. Choo-Smith, T. van Vreeswijk, H. P. Endtz, B. Smith, R. Bennett, H. A.  
1193 Bruining and G. J. Puppels, *Anal Chem*, 2000, **72**, 12-19.
- 1194 90. M. Harz, P. Rosch, K. D. Peschke, O. Ronneberger, H. Burkhardt and J. Popp, *Analyst*, 2005,  
1195 **130**, 1543-1550.
- 1196 91. E. C. Lopez-Diez and R. Goodacre, *Anal Chem*, 2004, **76**, 585-591.
- 1197 92. K. Maquelin, C. Kirschner, L. P. Choo-Smith, N. van den Braak, H. P. Endtz, D. Naumann and G.  
1198 J. Puppels, *J Microbiol Meth*, 2002, **51**, 255-271.
- 1199 93. D. Kusic, B. Kampe, P. Rosch and J. Popp, *Water Res*, 2014, **48**, 179-189.
- 1200 94. S. Meisel, S. Stockel, P. Rosch and J. Popp, *Food Microbiol*, 2014, **38**, 36-43.
- 1201 95. U. Münchberg, P. Rosch, M. Bauer and J. Popp, *Anal Bioanal Chem*, 2014, **406**, 3041-3050.
- 1202 96. A. Silge, W. Schumacher, P. Rosch, P. A. Da Costa, C. Gerard and J. Popp, *Syst Appl Microbiol*,  
1203 2014, **37**, 360-367.
- 1204 97. H. H. Wang, S. J. Ding, G. Y. Wang, X. L. Xu and G. H. Zhou, *Int J Food Microbiol*, 2013, **167**,  
1205 293-302.
- 1206 98. K. De Gussem, P. Vandenaabeele, A. Verbeken and L. Moens, *Spectrochim Acta A*, 2005, **61**,  
1207 2896-2908.
- 1208 99. U. Münchberg, L. Wagner, E. T. Spielberg, K. Voigt, P. Rösch and J. Popp, *Biochim. Biophys.*  
1209 *Acta, Mol. Cell Biol. Lipids*, 2013, **1831**, 341-349.
- 1210 100. E. W. Blanch, L. Hecht and L. D. Barron, *Methods*, 2003, **29**, 196-209.
- 1211 101. E. W. Blanch, I. H. McColl, L. Hecht, K. Nielsen and L. D. Barron, *Vib. Spectrosc.*, 2004, **35**, 87-  
1212 92.
- 1213 102. R. Tuma and G. J. Thomas, *Biophys Chem*, 1997, **68**, 17-31.
- 1214 103. Z. Q. Wen, S. A. Overman and G. J. Thomas, *Biochemistry-U.S.*, 1997, **36**, 7810-7820.
- 1215 104. Z. Q. Wen and G. J. Thomas, *Biopolymers*, 1998, **45**, 247-256.
- 1216 105. D. Dinakarparandian, B. Shenoy, M. PuztaiCarey, B. A. Malcolm and P. R. Carey, *Biochemistry-*  
1217 *Us*, 1997, **36**, 4943-4948.
- 1218 106. H. Peters, Y. Y. Kusov, S. Meyer, A. J. Benie, E. Bauml, M. Wolff, C. Rademacher, T. Peters and  
1219 V. Gauss-Muller, *Biochem J*, 2005, **385**, 363-370.
- 1220 107. P. Carmona, M. Molina and A. Rodriguez-Casado, *J Raman Spectrosc*, 2009, **40**, 893-897.
- 1221 108. A. Rodriguez-Casado, M. Molina and P. Carmona, *Appl Spectrosc*, 2007, **61**, 1219-1224.
- 1222 109. A. Rodriguez-Casado, M. Molina and P. Carmona, *Proteins*, 2007, **66**, 110-117.
- 1223 110. G. Font, M. J. Ruiz, M. Fernández and Y. Picó, *Electrophoresis*, 2008, **29**, 2059-2078.
- 1224 111. N. N. Brandt, A. Y. Chikishev, A. I. Sotnikov, Y. A. Savochkina, I. I. Agapov and A. G. Tonevitsky,  
1225 *J. Mol. Struct.*, 2005, **735-736**, 293-298.
- 1226 112. P. X. Zhang, Z. Xiaofang, Y. S. C. Andrew and F. Yan, *Journal of Physics: Conference Series*,  
1227 2006, **28**, 7-11.
- 1228 113. S. Bonora, E. Benassi, A. Maris, V. Tugnoli, S. Ottani and M. Di Foggia, *J. Mol. Struct.*, 2013,  
1229 **1040**, 139-148.
- 1230 114. G. D. Fleming, J. Villagrán and R. Koch, *Spectrochim Acta A*, 2013, **114**, 120-128.
- 1231 115. K. J. Leonard and W. R. Bushnell, *Fusarium head blight of wheat and barley*, MN: APS Press,  
1232 Saint Paul, 2004.
- 1233 116. J. E. Dexter, R. M. Clear and K. R. Preston, *Cereal Chem.*, 1996, **73**, 695-701.
- 1234 117. W. L. Casale, J. J. Pestka and L. P. Hart, *J Agr Food Chem*, 1988, **36**, 663-668.
- 1235 118. Y. Liu, S. R. Delwiche and Y. Dong, *Food Addit. Contam., Part A*, 2009, **26**, 1396-1401.
- 1236 119. K. M. Lee, T. J. Herrman and U. Yun, *J. Cereal Sci.*, 2014, **59**, 70-78.
- 1237 120. K.-M. Lee, J. Davis, T. J. Herrman, S. C. Murray and Y. Deng, *Food Chem*, 2015, **173**, 629-639.
- 1238 121. G. Gupta, A. S. B. Bhaskar, B. K. Tripathi, P. Pandey, M. Boopathi, P. V. L. Rao, B. Singh and R.  
1239 Vijayaraghavan, *Biosens. Bioelectron.*, 2011, **26**, 2534-2540.
- 1240 122. C. Sproll, W. Ruge, C. Andlauer, R. Godelmann and D. W. Lachenmeier, *Food Chem*, 2008,  
1241 **109**, 462-469.

- 1242 123. V. Sortur, J. Yenagi, J. Tonannavar, V. B. Jadhav and M. V. Kulkarni, *Spectrochim Acta A*, 2006,  
1243 **64**, 301-307.
- 1244 124. Y. Q. Huang, C. K. C. Wong, J. S. Zheng, H. Bouwman, R. Barra, B. Wahlström, L. Neretin and  
1245 M. H. Wong, *Environ. Int.*, 2012, **42**, 91-99.
- 1246 125. J. Dybal, P. Schmidt, J. Baldrian and J. Kratochvil, *Macromol.*, 1998, **31**, 6611-6619.
- 1247 126. T. G. Levitskaia, S. I. Sinkov and S. A. Bryan, *Vib. Spectrosc.*, 2007, **44**, 316-323.
- 1248 127. Z. Yu, L. A. Bracero, L. Chen, W. Song, X. Wang and B. Zhao, *Spectrochim Acta A*, 2013, **105**,  
1249 52-56.
- 1250 128. S. A. Asher, *Anal Chem*, 1984, **56**, 720-724.
- 1251 129. A. I. Alajtal, H. G. M. Edwards and I. J. Scowen, *J Raman Spectrosc*, 2011, **42**, 179-185.
- 1252 130. N. Sundaraganesan, N. Puviarasan and S. Mohan, *Talanta*, 2001, **54**, 233-241.
- 1253 131. I. V. Ermakov, M. R. Ermakova and W. Gellermann, *P Soc Photo-Opt Ins*, 2006, **6078**, 7835-  
1254 7835.
- 1255 132. E. Miranda-Bermudez, N. Belai, B. P. Harp, B. J. Yakes and J. N. Barrows, *Food Addit. Contam.,*  
1256 *Part A*, 2012, **29**, 38-42.
- 1257 133. M. Snehaltha, C. Ravikumar, N. Sekar, V. S. Jayakumar and I. H. Joe, *J Raman Spectrosc*,  
1258 2008, **39**, 928-936.
- 1259 134. N. Peica, I. Pavel, S. C. Pinzaru, V. K. Rastogi and W. Kiefer, *J Raman Spectrosc*, 2005, **36**, 657-  
1260 666.
- 1261 135. C. S. Mangolim, C. Moriwaki, A. C. Nogueira, F. Sato, M. L. Baesso, A. M. Neto and G. Matioli,  
1262 *Food Chem*, 2014, **153**, 361-370.
- 1263 136. K. Zborowski, R. Grybos and L. M. Proniewicz, *Vib. Spectrosc.*, 2005, **37**, 233-236.
- 1264 137. N. Peica, C. Lehene, N. Leopold, S. Schlucker and W. Kiefer, *Spectrochim Acta A*, 2007, **66**,  
1265 604-615.
- 1266 138. N. Peica, *J Raman Spectrosc*, 2009, **40**, 2144-2154.
- 1267 139. T. Jiang, R. James, S. G. Kumbar and C. T. Laurencin, in *Natural and Synthetic Biomedical*  
1268 *Polymers*, 2014, pp. 91-113.
- 1269 140. A. Zajac, J. Hanuza, M. Wandas and L. Dyminska, *Spectrochim Acta A*, 2015, **134**, 114-120.
- 1270 141. K. Zhang, J. Helm, D. Peschel, M. Gruner, T. Groth and S. Fischer, *Polymer*, 2010, **51**, 4698-  
1271 4705.
- 1272 142. M. C. Sarraguca, T. De Beer, C. Vervaet, J. P. Remon and J. A. Lopes, *Talanta*, 2010, **83**, 130-  
1273 138.
- 1274 143. R. M. El-Abassy, P. Donfack and A. Materny, *Food Chem*, 2011, **126**, 1443-1448.
- 1275 144. R. Goodacre, B. S. Radovic and E. Anklam, *Appl Spectrosc*, 2002, **56**, 521-527.
- 1276 145. M. Holse, F. H. Larsen, A. Hansen and S. B. Engelsen, *Food Res. Int.*, 2011, **44**, 373-384.
- 1277 146. M. M. Paradkar and J. Irudayaraj, *Food Chem*, 2002, **76**, 231-239.
- 1278 147. B. Özalci, I. H. Boyaci, A. Topcu, C. Kadilar and U. Tamer, *Food Chem*, 2013, **136**, 1444-1452.
- 1279 148. F. Corvucci, L. Nobili, D. Melucci and F.-V. Grillenzoni, *Food Chem*, 2015, **169**, 297-304.
- 1280 149. A. Keidel, D. von Stetten, C. Rodrigues, C. Mañãguas and P. Hildebrandt, *Journal of*  
1281 *Agricultural and Food Chemistry*, 2010, **58**, 11187-11192.
- 1282 150. A. B. Rubayiza and M. Meurens, *J Agr Food Chem*, 2005, **53**, 4654-4659.
- 1283 151. R. Korifi, Y. Le Dreau, J. Molinet, J. Artaud and N. Dupuy, *J Raman Spectrosc*, 2011, **42**, 1540-  
1284 1547.
- 1285 152. E. Guzmán, V. Baeten, J. A. F. Pierna and J. A. Garcia-Mesa, *Talanta*, 2012, **93**, 94-98.
- 1286 153. I. Gouvinhas, N. Machado, T. Carvalho, J. M. M. M. de Almeida and A. I. R. N. A. Barros,  
1287 *Talanta*, 2015, **132**, 829-835.
- 1288 154. H. M. Velioğlu, H. T. Temiz and I. H. Boyaci, *Food Chem*, 2015, **172**, 283-290.
- 1289 155. H. Mohamadi Monavar, N. K. Afseth, J. Lozano, R. Alimardani, M. Omid and J. P. Wold,  
1290 *Talanta*, 2013, **111**, 98-104.
- 1291 156. K. Czamara, K. Majzner, M. Z. Pacia, K. Kochan, A. Kaczor and M. Baranska, *J Raman*  
1292 *Spectrosc*, 2014, n/a-n/a.
- 1293 157. S. Sivakesava, J. Irudayaraj and A. Demirci, *J Ind Microbiol Biot*, 2001, **26**, 185-190.

- 1294 158. S. Sivakesava, J. Irudayaraj and D. Ali, *Process Biochem*, 2001, **37**, 371-378.
- 1295 159. R. S. Uysal, E. A. Soykut, I. H. Boyaci and A. Topcu, *Food Chem*, 2013, **141**, 4333-4343.
- 1296 160. Q. Y. Wang, Z. G. Li, Z. H. Ma and L. Q. Liang, *Sensor Actuat B-Chem*, 2014, **202**, 426-432.
- 1297 161. R. Rodriguez, S. Vargas, M. Estevez, F. Quintanilla, A. Trejo-Lopez and A. R. Hernández-Martínez, *Vib. Spectrosc.*, 2013, **68**, 133-140.
- 1298
- 1299 162. H. Lee, B.-K. Cho, M. S. Kim, W.-H. Lee, J. Tewari, H. Bae, S.-I. Sohn and H.-Y. Chi, *Sensor Actuat B-Chem*, 2013, **185**, 694-700.
- 1300
- 1301 163. J. Trebolazabala, M. Maguregui, H. Morillas, A. de Diego and J. M. Madariaga, *Spectrochim Acta A*, 2013, **105**, 391-399.
- 1302
- 1303 164. J. Qin, K. Chao and M. S. Kim, *J. Food Eng.*, 2011, **107**, 277-288.
- 1304 165. A. G. Gonzalez, D. Martin, K. Slowing and A. Gonzalez Ureña, *Food Struct.*, 2014.
- 1305 166. H. L. T. Lee, P. Boccazzi, N. Gorret, R. J. Ram and A. J. Sinskey, *Vib. Spectrosc.*, 2004, **35**, 131-137.
- 1306
- 1307 167. Y. Numata, Y. Shinohara, T. Kitayama and H. Tanaka, *Process Biochem*, 2013, **48**, 569-574.
- 1308 168. A. A. Argyri, R. M. Jarvis, D. Wedge, Y. Xu, E. Z. Panagou, R. Goodacre and G.-J. E. Nychas, *Food Control*, 2013, **29**, 461-470.
- 1309
- 1310 169. P. J. Li, B. H. Kong, Q. Chen, D. M. Zheng and N. Liu, *Meat Sci.*, 2013, **93**, 67-72.
- 1311 170. S. K. Oh, S. J. Yoo, D. H. Jeong and J. M. Lee, *Bioresource Technol*, 2013, **142**, 131-137.
- 1312 171. O. Abbas, P. Dardenne and V. Baeten, in *Chemical Analysis of Food: Techniques and Applications*, Academic Press, Boston, 2012, pp. 59-89.
- 1313
- 1314 172. M. Q. Zou, X. F. Zhang, X. H. Qi, H. L. Ma, Y. Dong, C. W. Liu, X. Guo and H. Wang, *J Agr Food Chem*, 2009, **57**, 6001-6006.
- 1315
- 1316 173. X. F. Zhang, M. Q. Zou, X. H. Qi, F. Liu, C. Zhang and F. Yin, *J Raman Spectrosc*, 2011, **42**, 1784-1788.
- 1317
- 1318 174. X. F. Zhang, X. H. Qi, M. Q. Zou and F. Liu, *Anal Lett*, 2011, **44**, 2209-2220.
- 1319 175. E. C. Lopez-Diez, G. Bianchi and R. Goodacre, *J Agr Food Chem*, 2003, **51**, 6145-6150.
- 1320 176. R. M. El-Abassy, P. Donfack and A. Materny, *J Raman Spectrosc*, 2009, **40**, 1284-1289.
- 1321 177. H. Yang and J. Irudayaraj, *J Am Oil Chem Soc*, 2001, **78**, 889-895.
- 1322 178. V. Baeten and R. Aparicio, *Biotechnol., Agron., Soc. Environ.*, 2000, **4**, 196-203.
- 1323 179. R. S. Uysal, I. H. Boyaci, H. E. Genis and U. Tamer, *Food Chem*, 2013, **141**, 4397-4403.
- 1324 180. Y. Cheng, Y. Y. Dong, J. H. Wu, X. R. Yang, H. Bai, H. Y. Zheng, D. M. Ren, Y. D. Zou and M. Li, *J Food Compos Anal*, 2010, **23**, 199-202.
- 1325
- 1326 181. S. Okazaki, M. Hiramatsu, K. Gonmori, O. Suzuki and A. T. Tu, *Forensic Toxicol*, 2009, **27**, 94-97.
- 1327
- 1328 182. G. P. S. Smith, K. C. Gordon and S. E. Holroyd, *Vib. Spectrosc.*, 2013, **67**, 87-91.
- 1329 183. J. Qin, K. Chao and M. S. Kim, *Food Chem*, 2013, **138**, 998-1007.
- 1330 184. M. M. Paradkar, S. Sakhamuri and J. Irudayaraj, *J Food Sci*, 2002, **67**, 2009-2015.
- 1331 185. X. Feng, Q. Zhang, P. Cong and Z. Zhu, *Talanta*, 2013, **115**, 548-555.
- 1332 186. I. H. Boyaci, H. E. Genis, B. Guven, U. Tamer and N. Alper, *J Raman Spectrosc*, 2012, **43**, 1171-1176.
- 1333
- 1334 187. D. Nguyen and E. Wu, *Spectroscopy-Us*, 2011, **26**, 95-95.
- 1335 188. J. R. Beattie, S. J. Bell, C. Borggaard, A. Fearon and B. Moss, *Lipids*, 2007, **42**, 679-685.
- 1336 189. K. Sowoidnich and H.-D. Kronfeldt, *Appl. Phys. B*, 2012, **108**, 975-982.
- 1337 190. I. H. Boyaci, H. T. Temiz, R. S. Uysal, H. M. Velioglu, R. J. Yadegari and M. M. Rishkan, *Food Chem*, 2014, **148**, 37-41.
- 1338
- 1339 191. İ. Boyaci, R. Uysal, T. Temiz, E. Shendi, R. Yadegari, M. Rishkan, H. Velioglu, U. Tamer, D. Ozay and H. Vural, *Eur Food Res Technol*, 2014, **238**, 845-852.
- 1340
- 1341 192. A. Zajac, J. Hanuza and L. Dymińska, *Food Chem*, 2014, **156**, 333-338.

1342

1343

1344 **FIGURE LEGEND**

1345

1346 Fig.1. Energy level diagram of Rayleigh and Raman scattering.

1347 Fig.2. Schematic presentation of fields in food analysis in which Raman spectroscopy used.

Figure 1.

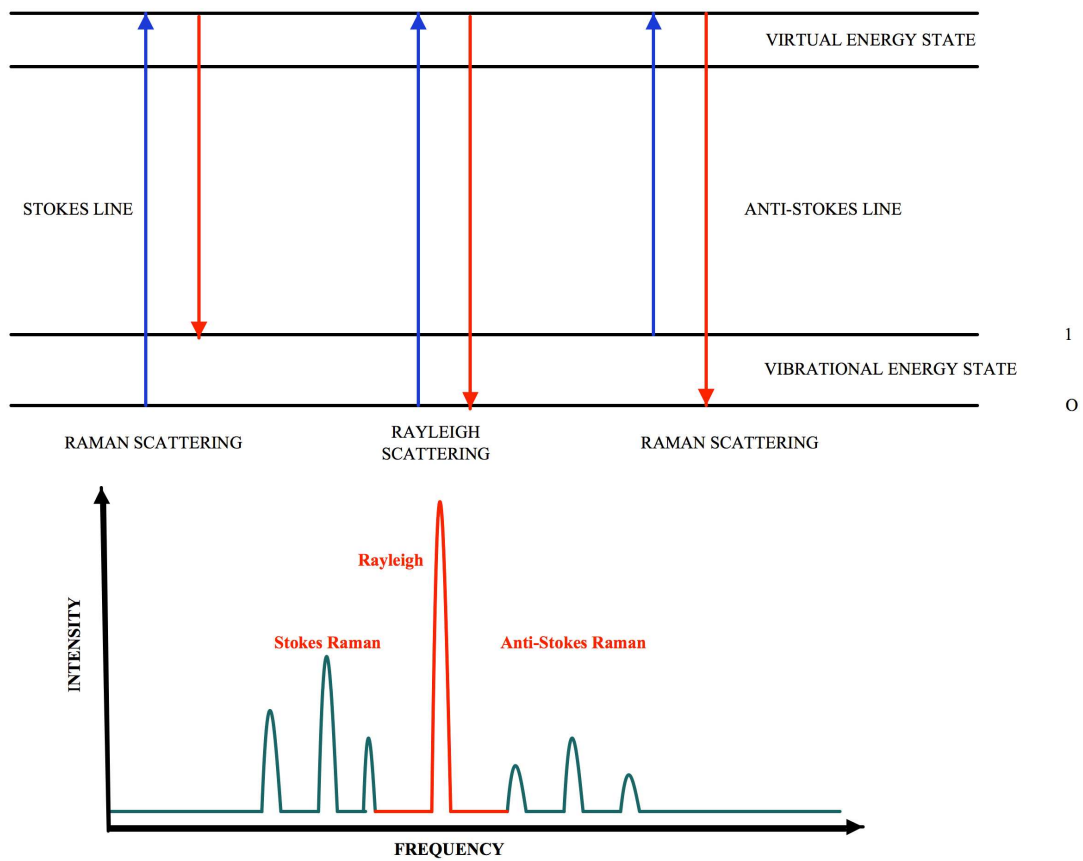


Figure. 2.

